IEEE Access
Multidisciplinary ⋮ Rapid Review ⋮ Open Access Journal

Received 6 February 2023, accepted 27 February 2023, date of publication 1 March 2023, date of current version 7 March 2023.

Digital Object Identifier 10.1109/ACCESS.2023.3250760

RESEARCH ARTICLE

Multi-Objective Optimal Siting and Sizing of Distributed Generators and Shunt Capacitors Considering the Effect of Voltage-Dependent Nonlinear Load Models

AAMIR ALI[1], GHULAM ABBAS[2], MUHAMMAD USMAN KEERIO[1], SOHRAB MIRSAEIDI[3], (Senior Member, IEEE), SHAHR ALSHAHR[4], AND AHMED ALSHAHIR[4]

[1]Department of Electrical Engineering, Quaid-e-Awam University of Engineering Science and Technology, Nawabshah, Sindh 67450, Pakistan
[2]School of Electrical Engineering, Southeast University, Nanjing 210096, China
[3]School of Electrical Engineering, Beijing Jiaotong University, Beijing 100044, China
[4]Department of Electrical Engineering, College of Engineering, Jouf University, Sakaka 72388, Saudi Arabia

Corresponding author: Sohrab Mirsaeidi (msohrab@bjtu.edu.cn)

This work was supported by the National Natural Science Foundation of China under Grant 52150410399.

ABSTRACT Load modeling is essential to distribution system analysis, planning, and control. Therefore, in this work, effect of non-linear load models has been considered for the optimal site and size of DG and SC allocation. A new and efficient modified branch and bus ordering-based forward-backward load flow method has been applied to solve load flow problem in radial distribution system. Recently implemented several state-of-the-art evolutionary algorithms (EAs) are employed to solve optimal site and size of DG and SC allocation problems and it is shown that performance of multi-operator/multimethod is better than other algorithms that are based on a single operator and/or algorithm. Therefore, a new hybrid EA based on various state-of-the-art operators such as GA, DE, and PSO is designed and applied to solve optimal site and size of DG and SC allocation problems. Various technical objective functions (index of active and reactive power loss and voltage deviation index) are considered to show the impacts of non-linear load models. From the simulation results, it is shown that DG and SC allocation problem is multi-objective. Therefore, further weighted sum multi-objective technical, economic, and environmental functions are formulated to find the solution to DG and SC allocation problems. The gathered results demonstrate that the proposed methodology significantly minimizes the cost of energy supplied by grid, total operating cost, and active and reactive power losses. Consequently, it can be stated that the suggested methodology has considerable economic and technological benefits and may be used to address many optimization issues in various distribution networks.

INDEX TERMS Distributed generation, shunt capacitor, distribution system, constrained evolutionary algorithm, non-linear load models.

I. INTRODUCTION

A. LITERATURE REVIEW

Current changes in the electric utility structure with the integration of distributed generation (DG) have created opportunities for many technological innovations to achieve a variety of technical and economic benefits such as; reduction in line losses, fuel cost, peak shaving, voltage deviation, emission (greenhouse gases), O&M cost, and enhancement in voltage level, over all energy efficiency, system reliability, power quality, security for critical loads. A maximum of above benefits in the distribution are obtained by integrating distributed generation (DG) of appropriate site and size that add local active and reactive power directly near distribution system.

The associate editor coordinating the review of this manuscript and approving it for publication was Qiang Li.

DGs operate at optimal power factor to minimize the active and reactive losses in the system. By adding reactive power to the system, shunt capacitor (SC) banks help with reactive power correction. Both DGs and SC banks, when placed in appropriate sites with the best sizes, may considerably improve quality of power, efficiency, and stability in addition to economic factors [1].

In the past few decades various optimization techniques were employed to find the optimal allocation of DGs and SCs, these include hybrid, evolutionary-based, and analytical methods. Many analytical techniques are used to resolve the DG allocation problem. Abdelkader et al. [2] proposed an iterative analytical formula for the DG allocation problems. The Multiobjective optimal DG allocation based on branch Loss Bus Injection Index (BLBII) analytical expressions are formulated and solved in [3]. Various objective functions proposed in BLBII formulation are active power loss, VD, energy not served, and VSI. A very simple analytical method to minimize active power loss for the optimal site and size is proposed in [4]. In the study, many DG characteristics were analyzed and examined, and various power considerations were taken into account. The authors in [5] employed an analytical approach for integrating the DG with distribution networks to reduce losses. Using the aggregated sum technique for multi-objective optimization, they evaluated their strategy on single and multiple DG allocations. Another research [6], which took into account the active and reactive current components of the DG, employed the analytical technique for distributing various DG units to reduce losses. The best outcomes are obtained when the approach first finds a series of potential buses and then chooses the size of the DGs. Similar studies based on various analytical expressions can be found in [7], [8], and [9] with different objectives, test systems, and analyses as shown in Table 1.

Numerous literary works that merged the individual SC, DG, or a combination of the two did so using heuristic or metaheuristic optimization methodologies. For grid-connected and islanded micro-grid systems, fixed and switchable capacitors are optimized in [10] using a spotted hyena optimizer (SHO). The gravitational search algorithm (GSA) and sensitivity analysis are used to study the allocation of SC banks in [11] to reduce the annual cost of system losses and SC installation. The expenses of running and maintaining SCs deployed in RDS are not included in that analysis. To locate and determine the magnitude of the DGs and SCs concurrently in distribution systems, the intersect mutation differential evolution (IMDE) method [1] was developed. The goal was to minimize power loss and associated expenses. As part of a MOO approach utilizing the aggregates sum technique, both DG-SC is optimized in [12] using the constriction-factor particle swarm optimization (Cf-PSO). Recent research in [13] focused on DSTATCOM size and positioning in radial distribution systems to decrease losses, raise the voltage level, and maximize the voltage stability index (VSI) under diverse variable demands using whale optimization algorithms (WOA). Ali et al. in [14] appropriately sized solar (PV) type DG and energy storage system (ESS) coupled to distribution network using fuzzy logic and chaotic slap swarm algorithm (CSSA). To maximize the VSI and minimize power losses and VD, the researchers applied their approach for multi-objective optimization. Optimal allocation of various DG units using enhanced GA (EGA) was suggested in [15] to accomplish various objective functions. The multi-objective optimization issue was addressed by the authors using a variety of strategies that includes the weighted sum approach, epsilon constraint method and Pareto Front based. The goals were to minimize active power loss, and VD whereas, maximizes VSI. The DG allocation problem in distribution system was solved using grey wolf optimization (GWO) in [26] to minimize system losses and improve the voltage profile. To minimize losses while improving voltage profile and system stability, an improved artificial eco-system based optimization (EAEO) [27] is developed and applied to single and multi-objective problems.

Two different variants of PSO were created in [25] to address the solution of DG allocation problem. These variants referred to as adaptive and exponential PSO were compared in terms of how well they improved distribution system. The GA was implemented in [24] to manage various capacitors and shunt reactors and maximized reactive power in real-time applications. The improved decomposition-based EA (I-DBEA) in [21] and Manta Ray foraging optimization (MRFO) were implemented in [23] and are employed to solve Multi-objective DG integration into distribution problems to minimize VD and losses and maximize VSI. Some metaheuristic algorithms that include harmony search algorithm (HAS) [20], water cycle algorithm (WCA) [19], multi-objective evolutionary algorithm based on decomposition (MOEA/D) [18], non-dominated sorting GA (NSGA) in [17], and intersect mutation differential evolution (IMDE) [1] have been used for finding DG and SCBs allocation. Table 1 explicitly shows the crux of the literature review.

The optimal allocation of DG and SC can highly improve performance and efficiency of distribution system. Integration of reactive power of SCs, at optimal site and size, can also improve power factor of distribution system and hence improve voltage profile of system.

Load modeling has a significant impact on power system studies. Load modeling has received more attention in recent years because of renewable integration, demand-side management, and smart metering devices. However, Table 1 clearly shows that the commonly used constant PQ type load model is widely studied for the DG and SC allocation. In [31], [33], and [34], a thorough analysis of the load model to be applied for power flow and dynamic studies is offered. Authors in [35] and [36] experimentally showed the impact of load models in planning studies in terms of appropriate capacitor placement/switching. According to the authors' analysis, switching a capacitor bank to increase the power factor was

TABLE 1. Crux of the literature review.

Year/Method/Ref	Test System	Single/Multi	Objective Function	Type	Load Model
2013/AM/[16]	69-bus	Single	P_{loss}	DG	PQ
2014/AM/[8]	33/69-bus	Single	P_{loss}	DG	PQ
2010/AM/[9]	16/33-bus	Single	P_{loss}	DG	PQ
2015/AM/[6]	15/33-bus	Single	P_{loss},	DG	PQ
2015/AM/[5]	33/69-bus	Single	P_{loss},	DG	PQ
2019/AM/[2]	33/69-bus	Single	P_{loss},	DG	PQ
2019/AM/[4]	12/33/69-bus	Single	P_{loss},	DG	PQ
2019/AM/[3]	33/85-bus	Multiobjective	P_{loss}, VD, VSM, ENS	DG	PQ
2016/IMDE/[1]	33/69-bus	Single	P_{Loss}, Q_{Loss}	DG/SC	PQ
2016/NSGA/[17]	28-bus	Multi	VD and Q_{SC}	DG/SC	PQ
2017/MOEAD/[18]	33/69/119-bus	Multi	P_{loss}, VD	DG/SC	PQ
2018/WCA/[19]	33/69-bus	Single/Multi	P_{loss}, VD, VSI and Cost	DG/SC	PQ
2013/HAS/[20]	33/69-bus	Single	P_{loss}, VD	DG	PQ
2021/I-DBEA/[21]	33/69/119-bus	Multi	P_{loss}, VD and VSI	DG	PQ
2022/JSA/[22]	69/136-bus	Single/Multi	Cost, P_{loss}, VD and VSI	DG/SC	ZIP, RES, COM, IND
2020/MRFO/[23]	33/ 69-bus	Single	P_{loss}, VD and VSI	DG	PQ
2020/GA/[24]	18-bus	Single	Q_{loss}	SC	PQ
2021/PSO/[25]	33/37-bus	Multi	P_{loss}, VD and VSI	DG	PQ
2020/GWO/[26]	16/30/57/118-bus	Single	P_{loss}	DG	PQ
2020/EAEO/[27]	33/69/119-bus	Single	P_{loss}, VD and VSI	DG	PQ
2020/EGA/[15]	33/69/119-bus	Single	P_{loss}, Q_{Loss} and VD	DG/SC	PQ
2021/WOA/[13]	33/69-bus	Multiobjective	P_{loss}, VD and reliability	DSTATCOM	RES, COM, IND
2020/CSSA/[14]	33/94-bus	Multiobjective	P_{loss}, VD and VSI	DG/ESS	PQ
2015/GSA/[11]	33/69/85-bus	Single	CEL, C_{SC}	SC	PQ
2006/ES/[28]	9/34-bus	Multiobjective	ILP, ILQ, IVD, IC, IVR and ISC	DG	PQ
2005/GAMS/[29]	9-bus	Single	Cost	DG	PQ
2004/ES/[30]	9/12-bus	Single	VPII, LLRI, EIRI, BI	DG	PQ
2007/ES/[31]	38-bus	Single	ILP, ILQ, IVD and IC	DG	RES, COM, IND
2003/MCS/[32]	10-bus	Single	AUL*	DG	PQ
2021/SHO/[10]	24-bus	Single	P_{loss}, CEL, CSC	DG/SC	ZIP
2020/Cf-PSO/ [12]	33/136-bus	WSMO	P_{loss}, Q_{Loss}, VD and VSI, CEL, C_{TOT}	DG/SC	PQ

AUL: Average Unsupplied Load; VPII: Voltage profile improvement index; LLRI: line loss reduction index, EIRI: Environmental impact reduction index; BI: Benefit index (composite of VPII, LLRI, EIRI), CEL: Cost of Energy loss, CSC: Cost of Shunt capacitor, WSMO: Weighted sum multi-objective

predicted to reduce real and reactive power injections at the substation since feeder load was modeled as a steady power source. There is an increase in the measured active and reactive power injections. Utilizing a voltage-sensitive load model [35] to analyze the experimental data, it was shown that while feeder losses are decreased as a result of the placement of the capacitor, the improvement in voltage profile that follows causes an increase in loads that outweighs the loss reduction. The positioning of DGs in an optimization setting is comparable to the placement of capacitors previously addressed. Most of the planning methods invariably use power flow programs which normally utilize constant real and reactive power load model representation. It is observed from the literature review that load models are not included in planning the location and size, and calculating the said indices except in [22] who have considered the load model. Moreover, DG allocation problem must be considered multi-objective function to assess the benefits of adding renewable DG to the distribution system.

B. MOTIVATIONS

Direct implementation of FBS load flow results in poor convergence in residential, industrial, and commercial load models. Also, the direct FBS method consumes more time in simultaneous DG and SC allocation. Most of the authors in the literature consider constant PQ load model only that computes an unrealistic DG and SC site and size.

Moreover, most of the studies do not include the technical, economic, and environmental objective functions during optimal siting and sizing of simultaneous DG and SC allocation. However, even though it represents four different types, the majority of authors only take into account one model of the DG unit. Very few studies, such as [22], [37], [38], and [39], employed three or four load models when assigning DG units utilizing various optimization strategies. Most authors consider only a single objective function for the optimal site and size of DG/SC allocation problems. The aforementioned drawbacks motivate the author to (i) generalize distribution system modeling rather than relying on the fixed or constant

PQ load model reported in the studies above, (ii) take into account various objectives within the same study to address various critical parameters, (iii) highlight the cost of DG and SC devices for overall operating cost, and (iv) consider different types for the DG unit to generate active and reactive power.

C. CONTRIBUTIONS

In this work, all six types of nonlinear load models and practical mix load model are considered, including the constant-PQ (PQ), constant-current (CI), constant-impedance (CZ), industrial (IND), commercial (COM) and residential (RES) loads. These models depend on a nonlinear relationship between the demand and the bus voltage profile. To solve the distribution systems, modified network bus and branch ordering with forward and backward sweep (FBS) method are adopted. State of the art evolutionary algorithm has been implemented for the DG and SC allocation problem. From the advantages of different algorithms efficiently solving various DG and SC allocation problems, it is suggested that the Hybrid algorithm is the best choice to solve such problems. It is because GA has better exploration, PSO has better convergence speed and DE can handle integer-based constraints simply using a round operator. Therefore, a new hybrid algorithm along with the representative constraint handling technique is designed and implemented to solve proposed DG and SC allocation problem. In this work, single and multi-objective functions are considered to solve proposed problem. To show the superiority and performance of proposed method hybrid EA along with the integration of representative CHT and modified FBS load flow techniques, very small to large scale distribution systems (33, 69, and 118 bus test systems) are considered.

Moreover, the study includes an analysis of cost of DG and SC and the total operating cost and cost of emission. Finally, the capability of the hybrid GA-DE and PSO along with CHT is compared with the state-of-the-art EAs in solving such nonlinear optimization problems and is checked through statistical analysis showing its performance in terms of different statistical indicators. The main contribution made by this research is summarized as follows.

1. An efficient distribution network-based modified bus and branch order FBS load flow algorithm is applied.
2. A new hybrid Evolutionary algorithm along with representative constraint handling techniques is designed to solve DG and SC allocation problems.
3. The effects of different nonlinear composite load models considered in distribution systems to integrate optimal site and size of DG and SC are investigated.
4. Various conflicting objective functions such as yearly cost of energy supplied by substation, the cost of DG and SC units, and the total operating cost are considered to find the optimal DG and SC allocation.
5. The Hybrid GA-DE-PSO along with representative CHTs is adopted to solve a single and multi-objective optimization problem consisting of three sub-objectives using aggregated sum technique.
6. Statistical analysis is performed to quantify the capability of the proposed algorithm for solving such optimization problems.

In the remaining sections, section II implements composite non-linear voltage-dependent load models and an illustrative example of the radial distribution network for the FBS Load flow techniques where problem formulation is outlined in section III. In Section IV state-of-the-art EAs are applied to explore the competencies of the EAs to solve DG and Sc allocation problems into 33, 69, and 118 bus test systems. Also, in section IV hybrid proposed algorithm and constraint handling techniques are modeled. Analysis and comparison of simulation results are given in Section V. The main conclusion points are drawn in section VI.

II. NONLINEAR VOLTAGE DEPENDENT COMPOSITE LOAD MODELS AND LOAD FLOW METHOD

A. VOLTAGE-DEPENDENT COMPOSITE LOAD MODEL

To quantify the effect of various load models, 33, 69, and 118 node distribution systems are adopted. The data for p.u. line impedances, load data, and the line MVA limits are given in [40]. The effects of selected nonlinear voltage-dependent composite load models are investigated in different planning scenarios (test cases). In this work, load models can be mathematically expressed as

$$P_i = P_{0i}\left(c_1|\overline{V}|^0 + c_2|\overline{V}|^1 + c_3|\overline{V}|^2 + c_4|\overline{V}|^{0.18} + c_5|\overline{V}|^{0.92} + c_6|\overline{V}|^{1.51}\right) \quad (1)$$

$$Q_i = Q_{0i}\left(d_1|\overline{V}|^0 + d_2|\overline{V}|^1 + d_3|\overline{V}|^2 + d_4|\overline{V}|^6 + d_5|\overline{V}|^{4.04} + d_6|\overline{V}|^{3.40}\right) \quad (2)$$

whereas, P_{0i} and Q_{0i} are the real and reactive demand at nominal voltage, P_i and Q_i are the real and reactive power injection at bus i, parameters (c_1, d_1), (c_2, d_2), (c_3, d_3), (c_4, d_4), (c_5, d_5), and (c_6, d_6) are the compositions of PQ, CI, CZ, IND, COM and RES non-linear voltage dependent load models respectively. While in all composite load models, $\sum_{i=1}^{6} c_i$ and $\sum_{i=1}^{6} d_i$ must be equal to 1. In this paper, a composition of MIX load models is considered as;

25% of PQ ($c_1 = d_1 = 0.25$); and share of all the other loads are 15% i.e., ($c_1 = d_1 = c_2 = d_2 = c_3 = d_3 = c_4 = d_4 = c_5 = d_5 = c_6 = d_6 = 0.15$). Figure 1 shows an increase of active and reactive power injection at load due to the change in voltage between 0.95 to 1.05 p.u. The figure shows that at exactly 1p.u load bus voltage injects same active and reactive power in all the load models. Whereas, load bus voltage below 1p.u minimum active power injection into the CZ load (90% load demand), however, maximum injection into the IND (99% of active demand) on the other hand above 1p.u load bus voltage, maximum power injected into the CZ load bus (110% of PQ load) and minimum power injection into the IND load bus (101% of PQ load). In reactive power injection, load bus voltage below 1p.u, minimum reactive power injection into the industrial (approximate 75%) load model, however,

maximum injection in case of CI (95% load constant PQ). At the above 1p.u load bus voltage, maximum reactive power is injected to the IND load bus (more than 130% of PQ load), and minimum power is injected to the CI bus (105% of PQ load).

B. EFFICIENT FBS LOAD FLOW METHOD FOR THE NONLINEAR LOAD MODELS

For the efficient and fast FBS load flow, it is desirable to modify branch and bus order proposed in [41] i.e., number branches with numbers that are equal to the receiving bus numbers and sending bus numbers should be smaller than the receiving bus number. To demonstrate how the proposed branch ordering algorithm is easy to understand by considering an illustrated example of 15 bus radial distribution network as shown in Figure 2 (a). In this method initially two empty variables i.e., bus_order and branch_order is created. After that, the reference bus number (bus 1 in our case) is directly inserted in the bus_order and search bus_order entity in the from bus (f) column as shown in Table 2. Next, insert the corresponding entity of *to* bus (t) column and branch # are inserted in the bus_order and the branch_order respectively. The process is continued until all the buses and branches are inserted in the bus_order and branch_order. Modified new bus and branch indexes are shown in columns 6 and 8 of Table.

The modified network based on a new branch and bus indexes is shown in Figure 2 (b). Moreover, as shown in Figure 2 (c), an extra fictitious branch between reference bus 1 and fictitious zero buses is inserted to increase each branch number by 1. Finally, *indices of the sending nodes* of branches are stored in vector F such that $i = fk$. The modified network vector F and branch number shown in Table 3, offer an easy way to follow the path between any bus and reference bus.

For example, if we consider bus 15 (indicated green in Table 3) of Figure 2 (c), then path to the slack bus consists of bus 15, 12, 10, 3, 2, and 1 the following branches: considered bus 15 is the receiving bus, in proposed method receiving bus is the branch number, therefore, branch $i_{15} \longrightarrow F_{12} \longrightarrow i_{12} \longrightarrow F_{10} \longrightarrow i_{10} \longrightarrow F_3 \longrightarrow i_3 \longrightarrow F_2 \longrightarrow i_2 \longrightarrow F_1 \longrightarrow i_1$.

Tracing of path visibly shows that During path trace from bus 15 (only the colored branches and their associated receiving bus numbers are operated) to reference, therefore, overall search space complexity is highly reduced. For the illustration of FBS method a branch k, between bus i and k of modified radial distribution system is as shown in Figure 3, is considered.

The FBS approach entails five steps. Set iteration counter t=*1* and all bus voltages to 1p.u initially in step 1. Receiving end branch flow S_k^t) is calculated in step 2 as follows:

$$S_k^t = S_{Lk} - (P_{DGk} + jQ_{SCCk}) + (Yk)^* \times v_k^2, \quad k = 1, 2, \ldots, n \tag{3}$$

whereas; S_k^t and S_{Lk} are the complex power drawn by receiving end bus k and the load on bus k, P_{DGk} and jQ_{SCk} are the DG and SC injections at bus k, $(Yk)^* \times v_k^2$ is the power injected into the shunt branch component. In the third step, first to compute power at far end bus S_k^f as;

$$S_k^f = S_k^t + Z_s^k \left| \frac{S_k^t}{v_k} \right|^2 \quad k = n, n-1, n-2, \ldots, 2 \tag{4}$$

After that, sending power of branch k is added to the receiving power of the branch whose index is equal to $i = fk$ as:

$$S_i^t = S_{Li} + S_k^f \tag{5}$$

In the fourth step, sending end bus voltage V_i is computed as;

$$V_k = V_i - Z_s^k \left| \frac{S_k^f}{V_i} \right|^* \tag{6}$$

Finally in the fifth step, check the termination condition as

$$\left| V_i^t - V_i^{t-1} \right| < 10^{-8} \tag{7}$$

If Eq. (7) is true, terminate the condition, else go to step 2 and continue.

III. PROBLEM FORMULATION

DG and SC planning problem formulation is classified as mixed integer nonlinear programming (MINLP). During problem formulation, the following assumptions were made.

- ➢ DG units are operating at a constant power factor or near unity. In this study, DG units are assumed to operate at a unity power factor [1].
- ➢ Dispatchable inverter-based DGs are considered.
- ➢ Both DG and SC capacities are continuous.

Optimal DG allocation is a constrained optimization problem (COP) and without loss of generality COP can be described as:

$$\begin{aligned} &\min_{\vec{x}} f(\vec{x}), \vec{x} = (x_1, \ldots, x_D) \in S \\ &\quad L_i \le \vec{x}_i \le U_i \\ &s.t. \begin{cases} g_j(\vec{x}) \le 0, & j = 1, \ldots, l \\ h_j(\vec{x}) = 0, & j = l+1, \ldots m \end{cases} \end{aligned} \tag{8}$$

$\vec{x}_i$ is the i^{th} decision vector, D is the number of decision variables, L_i and U_i are the lower and upper bounds of i^{th} decision variable, $S = \Pi_{i=1}^{D} [L_i, U_i]$ denotes the feasible decision space, $f(\vec{x})$ is the objective function, $g_j(\vec{x})$ and $h_j(\vec{x})$ are the l and m inequality and equality constraints. DG and SC allocation extensively depends on the selection of objective function and constraint-handling techniques (CHT). The proposed method aims to achieve three types of objective functions these are technical, economic, and environmental.

A. TECHNICAL OBJECTIVE FUNCTIONS

In this work, three non-normalized indices of technical objective functions are considered to show the impact of voltage-sensitive nonlinear composite load models [31].

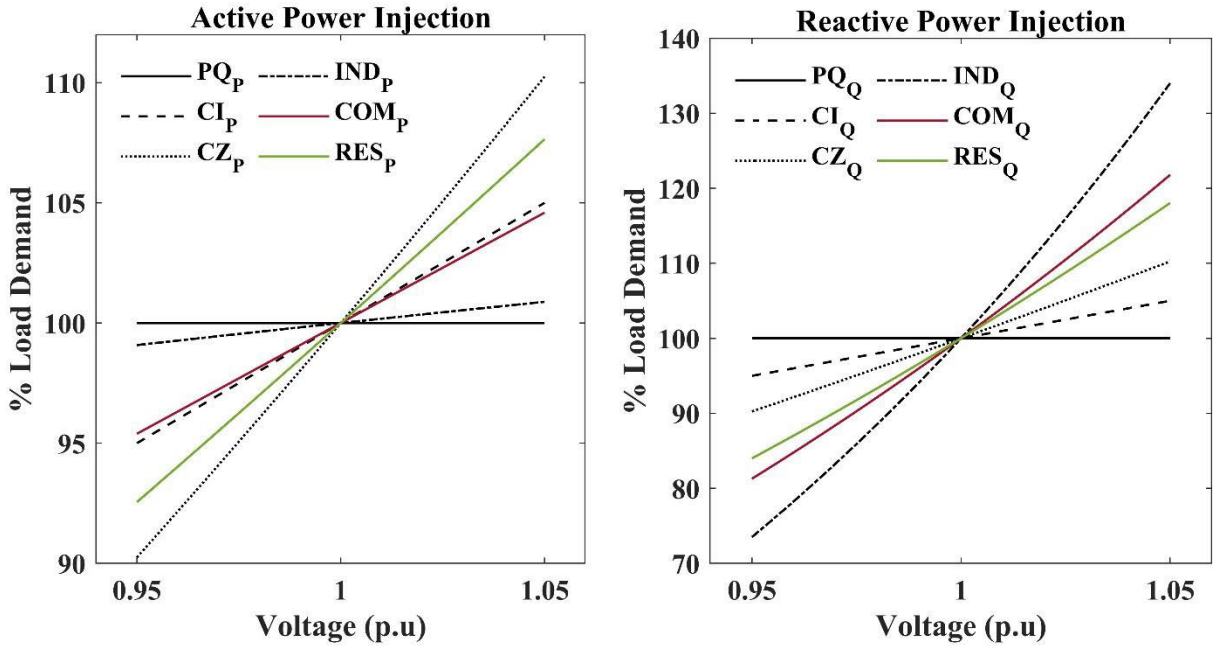

FIGURE 1. Active and reactive load bus injection subject to change in bus voltage magnitude in p.u.

TABLE 2. Formation of bus and branch order of 15-bus radial distribution network.

Buses	Branch #	f	t	Bus_order	New bus Index	Branch_order	New branch index
1 (ref)				1 (ref)	1		
2	1	1	2	2	2	1	1
3	2	2	3	3	3	2	2
4	3	3	4	6	4	7	3
5	4	4	5	9	5	5	4
6	5	2	9	4	6	3	5
7	6	9	10	7	7	8	6
8	7	2	6	8	8	9	7
9	8	6	7	10	9	6	8
10	9	6	8	11	10	10	9
11	10	3	11	5	11	4	10
12	11	11	12	12	12	11	11
13	12	12	13	14	13	13	12
14	13	4	14	15	14	14	13
15	14	4	15	13	15	12	14

TABLE 3. Branch number and sending end buses of illustrative example and Color shows the Tracing of path from bus 15 to reference bus.

Branches	1	2	3	4	5	6	7	8	9	10	11	12	13	14	15
F	0	1	2	2	2	3	4	4	5	3	6	10	6	6	12

1) REAL AND REACTIVE POWER LOSS INDICES (ILP AND ILQ)

The real and reactive power loss indices are defined as:

$$f_1 = \frac{[P_{LDG}]}{[P_L]} \times 100 \tag{9}$$

$$f_2 = \frac{[Q_{LDG}]}{[Q_L]} \times 100 \tag{10}$$

P_{LDG} and Q_{LDG} are the active and reactive power with DG, P_L and Q_L are the active and reactive power loss without DG. The lower the values, the better the benefits in terms of active and reactive power loss reduction accrued to DG location and size.

2) VOLTAGE PROFILE INDEX (IVD)

It is related to the maximum voltage drop which, in this case, considers the maximum drop between each node and the root node. This index could also be used to find prohibitive locations for DG considering preestablished voltage drop limits. In this way, the lower the index, the better the network

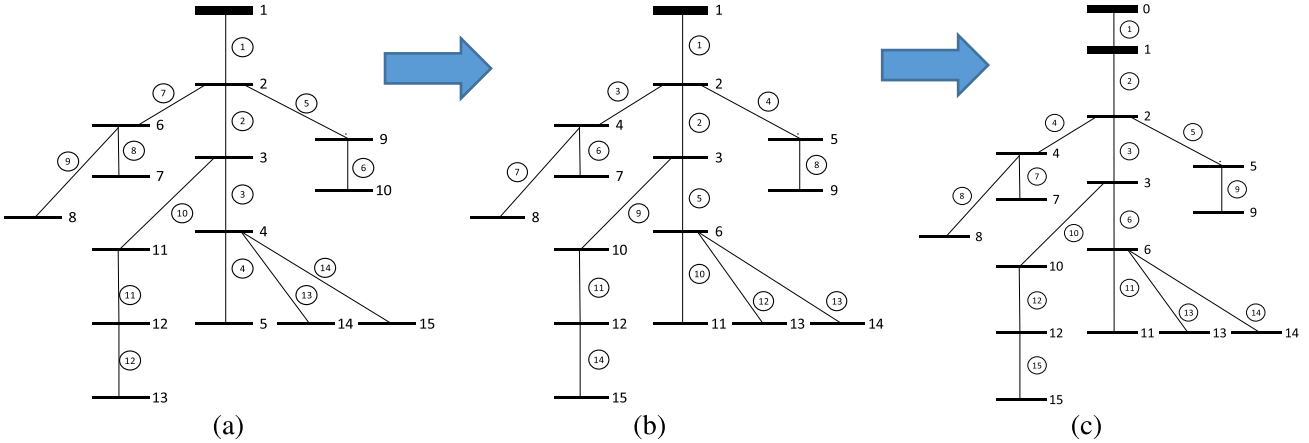

FIGURE 2. (A). Proposed 15-bus network. (B). Modified 15-bus network using new bus and branch indexes. (C). Increase each branch number by insertion of Fictitious branch.

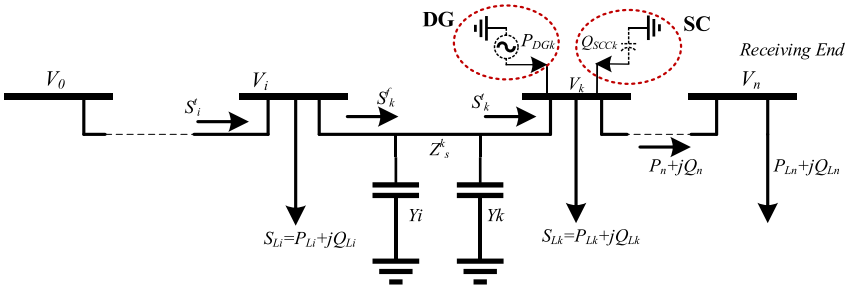

FIGURE 3. Representation of k^{th} branch between buses i and k.

performance. The IVD can be defined as follows:

$$f_3 = 100 \times max_{i=2}^{n}\left(\frac{|\overline{V}_1| - |\overline{V}_i|}{|\overline{V}_1|}\right) \tag{11}$$

whereas, $|\overline{V}_1|$ is the voltage magnitude of reference bus voltage and $|\overline{V}_i|$ voltage magnitude of load buses.

B. ECONOMIC OBJECTIVE FUNCTIONS

Deliberation of only technical objective functions are not an accurate representation of distribution company requirements but the cost of annual energy supplied by grid and DG and SC is the main factor that must be considered. Therefore, in this paper minimization of the overall cost of active power generation (C_{TOT}) [19] is considered one of the objective functions. C_{TOT} is computed as;

$$C_{TOT} = min\sum_{i=1}^{N_{DG}}(C_{SS} + C_{DG_i} + C_{SC}) \tag{12}$$

whereas, C_{SS}, C_{DG_i} and C_{CB} cost of power supplied by substation, DG, and SC, which is computed as,

$$C_{SS} = a \times P_{intake}\left(\frac{\$}{h}\right) \tag{13}$$

whereas, P_{inake} is the active power supplied by grid station and the parameter a ($/MWh) is 44 ($/MWh) taken from [43]. Cost of active power generated by DG (C_{DG_i}) is computed as;

$$C_{DG_i} = b + c * P_{DG_i}\left(\frac{\$}{h}\right) \tag{14}$$

where, P_{DG_i} is the active power injected by DG, the cost parameters b and c are 51.99 ($/h), 9.5 ($/MWh) respectively. Cost of reactive power supplied by shunt capacitors is computed as;

$$C_{SC} = \frac{\sum_{i=1}^{NC}(e_i + C_{ci}|Q_{ci}|)}{lifetime * 8760}\left(\frac{\$}{h}\right) \tag{15}$$

whereas, ei and Cci are the SC bank cost parameters equal to 1000 ($/h) and 30 000 $/MVArh, respectively taken from [44]. Figure 4 shows the comparison of cost of substation (C_{SS}), cost of DG (C_{DG}), cost of shunt capacitor (C_{SC}) and total cost (C_{TOT}) of the proposed nonlinear composite load models considering bus voltage variation between acceptable limit of 0.95 to 1.1 p.u. For the intuition of cost variation w.r.t to voltage-dependent load models, the x-axis shows the variation in voltage in (p.u), y-axis is the power injected by Substation (SS), DG, SC, or combination of these sources and z-axis is the cost of active or reactive power injection. The figure clearly shows that the cost is linear in PQ load models,

whereas, highly nonlinear in other load models. Above 1p.u voltage cost variation is increased highly, especially in green color (industrial load model) of capacitor cost.

C. ENVIRONMENTAL OF

Greenhouse gases (GHG) produced by CO_2, SO_2, and NO_x are considered as most effective pollutants. The mathematical formulation of this OF can be described as follows [9]:

$$E = \sum_{i=1}^{N_{DG}} \left(E_{DG_i} + E_{Grid}\right) \tag{16}$$

whereas,

$$E_{DG_i} = (CO_2^{DG_i} + NO_x^{DG_i} + SO_2^{DG_i}) \times P_{DG_i} \tag{17}$$

$$E_{Grid} = (CO_2^{Grid} + NO_x^{Grid} + SO_2^{Grid}) \times P_{gGrid} \tag{18}$$

In this study $E_{DG_i} = 0$.

1) MULTIOBJECTIVE FUNCTION

In this case, weighted sum multi-objective function [19] that is comprised of technical (active power loss), environmental and economic are combined. This objective function is defined as:

$$f_4 = 0.5 * P_L + 0.25 * Cost + 0.25 * E \tag{19}$$

whereas, during optimization, all the weighted objective functions are normalized for fair comparison.

2) EQUALITY CONSTRAINTS

$$\sum_{i=1}^{NG} P_{G_i} = P_D + P_{Loss} \tag{20}$$

$$\sum_{i=1}^{NG} Q_{G_i} = Q_D + Q_{Loss} \tag{21}$$

whereas, P_{G_i} and Q_{G_i} are the active and reactive injection, P_D and Q_D are the active and reactive load.

3) INEQUALITY CONSTRAINTS

During optimization Following inequality constraints are considered;

$$V_i^{min} \leq |V_i| \leq V_i^{max} \tag{22}$$

$$I_{ij} \leq I_{ij}^{max} \tag{23}$$

$$\sum_{i=1}^{N_{DG}} P_{DG,i} \leq P_{DG}^{max}, \quad \sum_{i=1}^{N_{DG}} Q_{DG,i} \leq Q_{DG}^{max} \tag{24}$$

$$\sum_{i=1}^{N_{DG}} P_{DG,i} \leq 0.9 * P_D,$$

$$\sum_{i=1}^{N_{DG}} Q_{DG,i} \leq 0.9 * P_D \tag{25}$$

$$\sum_{i=1}^{N_{SC}} Q_{SC,i} \leq 0.9 * Q_D \tag{26}$$

where, V_i^{min} and V_i^{max} are the minimum and maximum voltage at bus i. P_{DG}^{max} and Q_C^{max} are the maximum ratings of DG and SC,N_{DG} and N_{Sc} are the number of DGs and SCs, P_D and Q_D are the active and reactive power demand. However, installing DG units in the distribution network has a significant effect, as the network was originally planned for passive circuits. Improper allocation of DG units in the distribution system might lead to detrimental effects; therefore, the accommodation of high penetration of DG units in the power system has to be planned carefully through the allocation of DG units to maximize their benefits without violating constraints.

IV. PROPOSED OPTIMIZATION ALGORITHM

In the recent two decades, EAs were highly emphasized to solve constrained optimization problems (COPs). According to the no-free lunch theorem [45], none of them is universal, and a good understanding of the different methods is necessary to identify the most appropriate one in the context of specific applications. When solving COPs using evolutionary algorithms (EAs), the search algorithm plays a crucial role. In general, we expect that the search algorithm can balance not only diversity and convergence but also constraints and objective function during the evolution. Various state-of-the-art EAs have been applied to solve DG and SC allocation problems. It is found that GA [46] finds the best solution, whereas convergence speed is better found in PSO [47] and IMODE [48] strategy gives better trade-off between various operators for the exploration and diversity. Figure 5 shows the convergence curve of optimal site and size of DG and SC allocation of small to very large-scale radial distribution networks.

Figure 5 clearly shows that optimal DG and SC allocation problems in 33-bus and 69 bus effectively solved by GA [46], PSO [47], and IMODE [48]. PSO [47] has a higher convergence speed in 33 and 69-bus but it is stagnated in a locally optimal solution. The convergence speed of IMODE is slow but it explores the entire space. On the other hand, in a large-scale 118-bus distribution system, GA beats. GA attains better convergence compared to other state-of-the-art EAs. In most of the small and medium scale networks, performance of GA [46], SHADE [49], C^2oDE [50], and IMODE [48] have marginal differences. For this purpose, this paper offers a hybrid constrained evolutionary algorithm along with the integration of representative constraint handling techniques to effectively solve DG and SC allocation COP. Various operators of GA [46], DE [51], and PSO [47] are employed to generate offspring's have better exploration and exploitation properties for the solution of DG and SC allocation COP. In recent years, several multi-methods and multi-operator-based algorithms have been proposed for solving optimization problems. Generally, their performance is better than other algorithms that are based on a single operator and/or algorithm. However, they do not perform consistently well over all the problems tested in the literature [48].

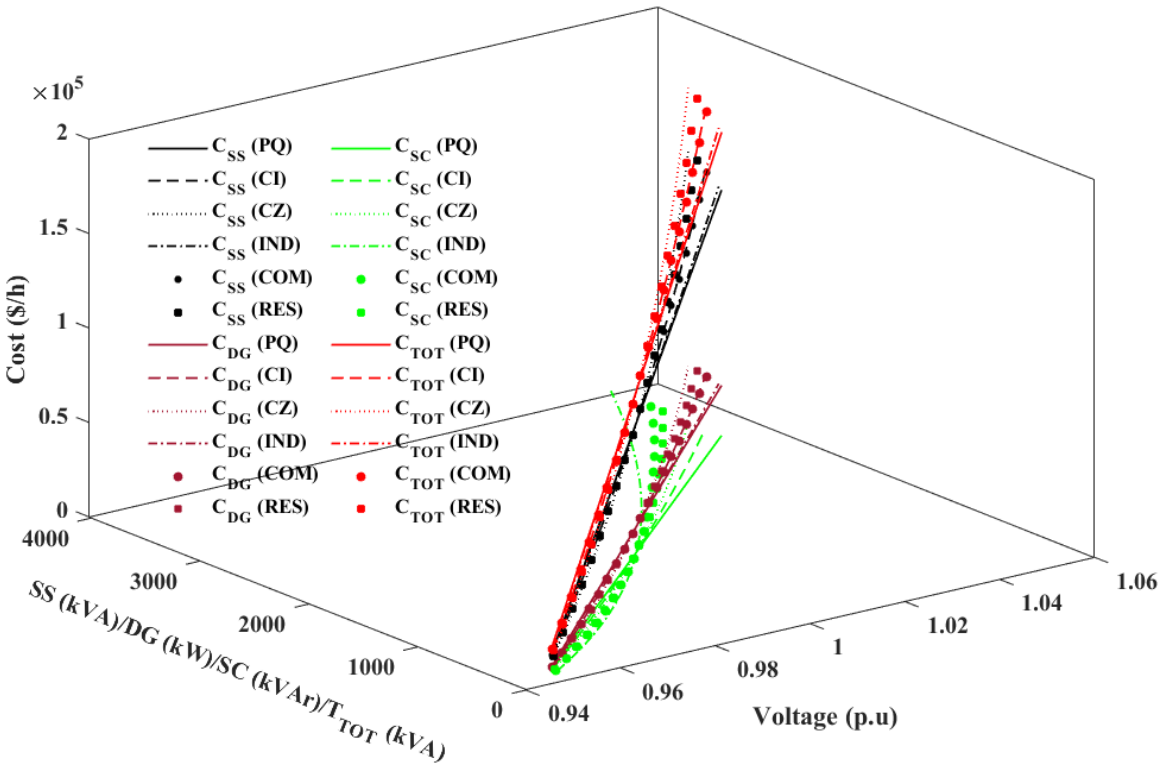

FIGURE 4. Cost of active and reactive power w.r.t bus voltage variation.

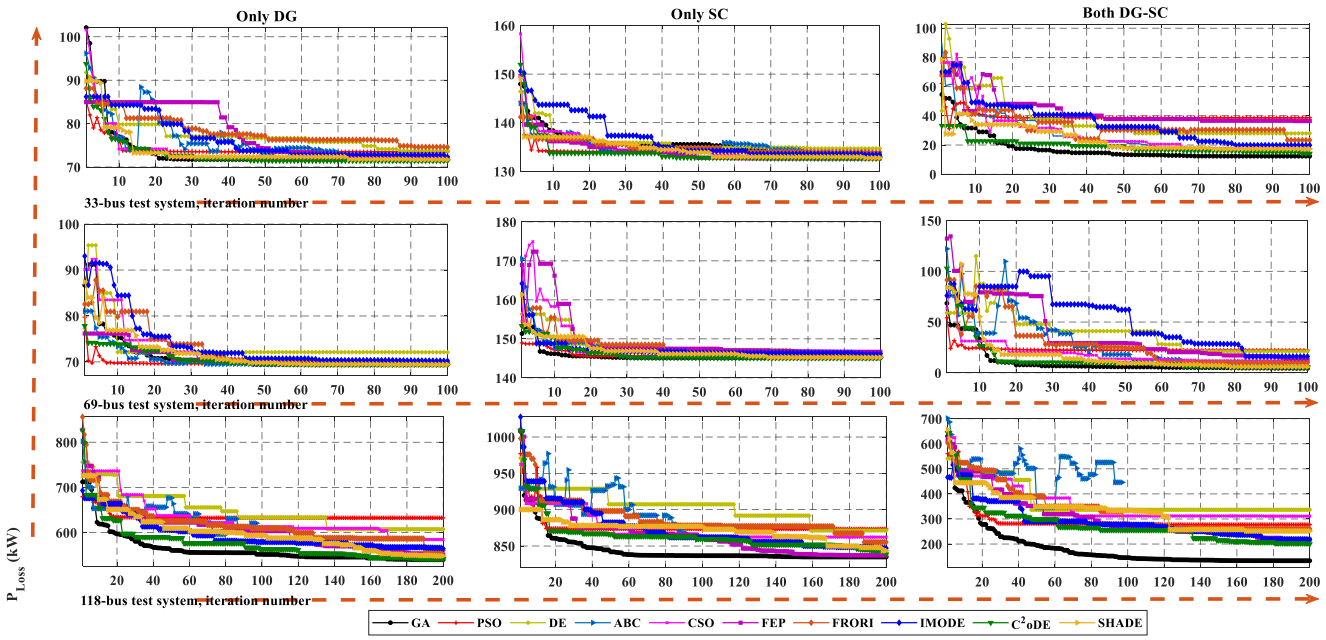

FIGURE 5. Convergence curve state-of-art EAs considering 33, 69, and 118-bus radial distribution system on constant PQ load model.

Therefore, in the proposed algorithm, three operators of GA, DE, and PSO are used to generate three vector strategies with distinct advantages. Specifically, crossover operators of GA are applied to obtain better convergence and two trail vector generation strategies of DE are employed to balance diversity and convergence. In addition, the velocity, local best, and global best of PSO operators are guided by GA and DE operators to tackle better convergence speed. During

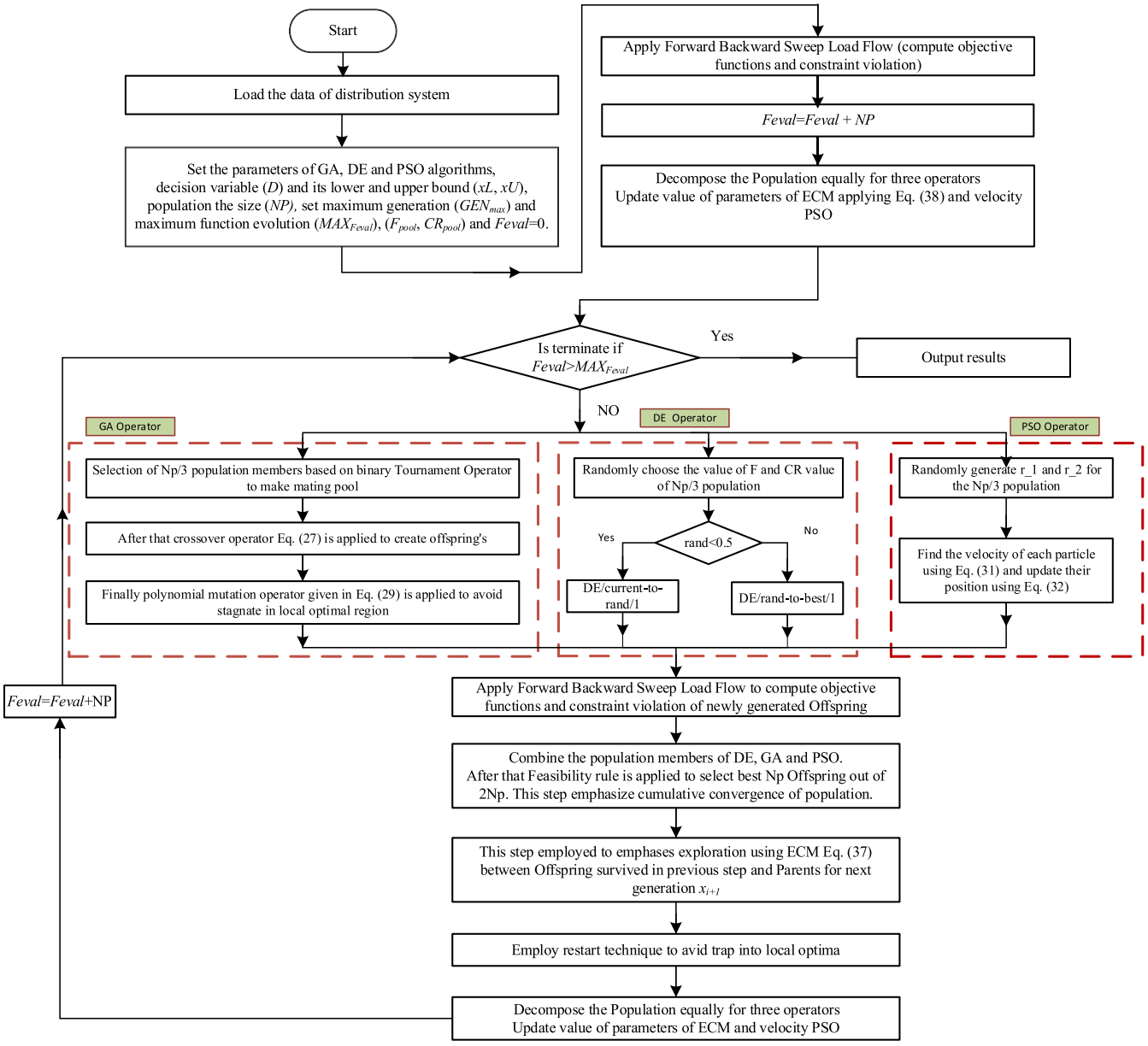

FIGURE 6. Flow chart for the implementation of proposed hybrid EAs.

evolution, these three operators are used to generate three offspring for each input vector. Afterward, the feasibility rule (emphasize the convergence) is employed to select Np offspring from 2Np. Selected NP offspring are compared with the parents using ECM (to employ trade-off between convergence and exploration) to select final Np population members for the next iterations. Here, FR is employed to preselect the best Np children generated by the proposed operators. Since the feasibility rule prefers constraints, the ε constrained method (ECM), which can incorporate the information of objective function to a certain degree, is used to compare each parent vector with its offspring vector. Therefore, the new comparison rule can further promote the balance between exploration and exploitation. Moreover, a restart scheme is designed to help the population jump out of a local optimum in the infeasible region for extremely complex problems. The flow chart of proposed hybrid GA-DE-PSO operators along with representative constraint techniques is shown in Figure 6.

After initialization and evaluation of objective functions, the population is decomposed into equal sections for each operator as described in [48]. In GA operator, binary tournament selection is employed to select 1/3 of initially generated population for mating pool. Then simulated binary crossover (SBX) operator [46] is applied to explore the search space. In SBX, two population members such as $\vec{x}_{r1}^{t}$ and $\vec{x}_{r1}^{t}$

are randomly selected to generate two offspring's $\vec{v}_1^t$ and $\vec{v}_2^t$ as

$$\vec{v}_1^t = \frac{1}{2}\left(\vec{x}_{r1}^t + \vec{x}_{r2}^t\right) - \frac{1}{2}\beta(\vec{x}_{r1}^t + \vec{x}_{r2}^t)$$
$$\vec{v}_2^t = \frac{1}{2}\left(\vec{x}_{r1}^t + \vec{x}_{r2}^t\right) + \frac{1}{2}\beta(\vec{x}_{r1}^t + \vec{x}_{r2}^t) \quad (27)$$

where β is called the spread factor and is computed as;

$$\beta_i = \begin{cases} (2 \times rand)^{\frac{1}{\eta_c+1}} & if\ rand \le 0.5; \\ \left(\frac{1}{2(1-rand)}\right)^{\frac{1}{\eta_c+1}} & otherwise. \end{cases} \quad (28)$$

Parameter η_c is the distribution index of SBX, $u_i \in [0, 1]$. Only the crossover operator may stagnate in the local optima. Therefore, a polynomial mutation operation with small probability is applied to enhance the exploration capability of algorithm. The polynomial mutation operator is given as

$$u_{i,j}^t = x_{i,j}^t + \left(x_{i,j}^{(U)} - x_{i,j}^{(L)}\right)\delta_i, \quad (29)$$

where, $x^{(U)}$ and $x^{(L)}$ are the lower and upper bounds of decision variable, and the parameter δ_i is given as;

$$\delta_i = \begin{cases} (2 \times rand)^{\frac{1}{\eta_m+1}} - 1 & if\ \ r_i < 0.5; \\ 1 - [2(1-rand)]^{\frac{1}{\eta_m+1}} & else \end{cases} \quad (30)$$

where, η_m is the distribution index and the operator *rand* is a random number generator. After GA operators, randomly selected 1/3 of the population members called *particles*, of the population are selected to apply PSO operator. PSO is a stochastic global optimization method inspired by the choreography of a bird flock. PSO relies on the exchange of information between individuals, called *particles*, of the population. In PSO, each particle adjusts its trajectory stochastically towards the positions of its own previously best performance (*pbest*) and the best previous performance of its neighbors or the whole swarm (*gbest*). At the t^{th} iteration, $\vec{v}_i^t = (v_{i,2}^t, \ldots, \vec{x}_{i,D}^t)$ shows the velocity of particle and $\vec{x}_i^t = (\vec{x}_{i,1}^t, \ldots, \vec{x}_{i,D}^t)$ is the position of a particle. The velocity and position updating rules at t+1 iteration are given as

$$v_{i,j}^{t+1} = \omega v_{i,j}^t + c_1 r_I \left(pbest_{i,j}^t - x_{i,j}^t\right) + c_2 r_2 \left(gbest - x_{i,j}^t\right) \quad (31)$$

$$x_{i,j}^{t+1} = x_{i,j}^t + v_{i,i}^{t+I} \quad (32)$$

where $j \in \{1, \ldots, D\}$, $\omega \in [0, 1]$ is the inertia factor, c_1 and c_2 are positive constants, r_1 and r_2 are two uniformly distributed random numbers in the range [0,1]. Here, the variable $\vec{v}_i^t$ is limited to the range $\pm V_{\max}$. When a particle discovers a position that is better than any it has found previously, it stores the new position as the corresponding *pbest*.

The rest of 1/3 population members generate offspring by employing similar strategies as given in [48]. The most widely used DE mutation operators are:

DE/rand/1

$$\vec{v}_i^t = \vec{x}_{r1}^t + F \cdot \left(\vec{x}_{r2}^t - \vec{x}_{r3}^t\right) \quad (33)$$

DE/rand/2

$$\vec{v}_i^t = \vec{x}_{r1}^t + F \cdot \left(\vec{x}_{r2}^t - \vec{x}_{r3}^t\right) + F \cdot \left(\vec{x}_{r4}^t - \vec{x}_{r5}^t\right) \quad (34)$$

DE/current-to-rand/l

$$\vec{v}_i^t = \vec{x}_i^t + F \cdot \left(\vec{x}_{r1}^t - \vec{x}_i^t\right) + F \cdot \left(\vec{x}_{r2}^t - \vec{x}_{r3}^t\right) \quad (35)$$

DE/rand-to-best/l

$$\vec{v}_i^t = \vec{x}_{r1}^t + F \cdot \left(\vec{x}_{best}^t - \vec{x}_{r2}^t\right) + F \cdot \left(\vec{x}_{r3}^t - \vec{x}_{r4}^t\right) \quad (36)$$

DE/current-to-best/l

$$\vec{v}_i^t = \vec{x}_i^t + F \cdot \left(\vec{x}_{best}^t - \vec{x}_i^t\right) + F \cdot \left(\vec{x}_{r1}^t - \vec{x}_{r2}^t\right) \quad (37)$$

where $\vec{x}_{r1}^t, \vec{x}_{r2}^t, \vec{x}_{r3}^t, \vec{x}_{r4}^t$ and $\vec{x}_{r5}^t$ are five mutually distinct target vectors randomly selected from the population, $\vec{x}_{best}$ is the best target vector in the current population, and rand is a uniformly distributed random number between 0 and 1. In this work, DE/current-to-rand/1 and DE/rand-to-best/1 can speed up the convergence. In DE/current-to-rand/1, each target vector learns from a randomly selected individual, thus promoting diversity. However, DE/rand-to-best/1 can push towards better solutions in the sense of convergence speed.

After producing offspring by the proposed operators, the feasibility rule and the ε constrained method (ECM) are combined elaborately for selection. In COP, after the effective generation of offspring, it is desirable to maintain population size to delete undesirable and infeasible solutions. Therefore, in the proposed algorithm, two representative constraint techniques are employed to select the survival of fittest particle at the end of each iteration. From the generation of 2Np offspring, feasibility rule (FR), which emphasizes the feasible solutions, is applied to select Np child solutions. In FR two children are randomly selected (say $\vec{u}_i$ and $\vec{u}_j$) and compare them as follows;

1) If both $\vec{u}_i$ and $\vec{u}_j$ are feasible, select the one which has a minimum objective function value.
2) If both $\vec{u}_i$ and $\vec{u}_j$ are infeasible, select the one which has minimum constraint violation.
3) If $\vec{u}_i$ is feasible and $\vec{u}_j$ is an infeasible, select feasible one.

To obtain better exploration epsilon constraint method (ECM) is employed to select the final population between parents and offspring for the next generation. In ECM let be assumed that $\vec{u}_i$ is superior to $\vec{x}_i$ at the selection stage if and only if the following conditions are satisfied

1. $f(\vec{u}_i) < f(\vec{x}_i)$, if $G(\vec{u}_i) < \mathcal{E}$ and $G(\vec{x}_i) < \mathcal{E}$
2. $f(\vec{u}_i) < f(\vec{x}_i)$, if $G(\vec{u}_i) = G(\vec{x}_i)$
3. $G(\vec{u}_i) < G(\vec{x}_i)$ (38)

whereas, parameter $\mathcal{E} = \mathcal{E}_o\left(1 - \frac{t}{T}\right)^{cp}$, if the ratio between current and maximum generation (t/T) is less than 50%, otherwise 0. However, $\mathcal{E}_o$ is the initial threshold and initially, it is equal to the maximum constraint violation. The parameter cp can be calculated as:

$$cp = -\frac{\log\varepsilon_0 + \lambda}{\log(1-p)}$$

where λ is set to 6 and p controls the exploitation of objective function. Moreover, a restart scheme is proposed to help the population jump out of a local optimum in the infeasible region for some extremely complicated DG and Sc allocation problems. By assembling the above techniques, a constrained hybrid EAs is proposed that combines the better properties of GA, DE, and PSO. In the proposed algorithm, the strategy for the selection of the operator is based on IMODE [48].

V. SIMULATION RESULTS

In the following subsections, first, compute the performance parameters of the proposed FBS method without DG and SC. Next, the performance and effectiveness of the proposed algorithm are statistically compared with the state-of-the-art EAs and the recent algorithms available in the literature.

Finally, the proposed technique is applied to the IEEE 33-bus and 118-bus systems to demonstrate the effects of realistic non-linear load models on various conflicting objective functions with the integration of DG, SC and simultaneous DG-SC.

A. DATA PREPARATION, TEST SYSTEMS, AN PERFORMANCE OF PROPOSED FBS METHOD WITHOUT DG

Total complex power load demand $(P_0 + jQ_0)$ for the 33, 69, and 118 bus systems are $3.715 + j2.300$, $3.802 + j2.695$, and $22.7097 + j17.04107$ respectively. In this subsection, all seven load models are simulated and resolved through the proposed FBS method, the effect of load models on the following studies was made:

1. $MVA_{sys}/S_{intake} = [(P_{intake})^2 + (Q_{intake})^2]^{1/2}$
2. $P_{intake} = real(S_{intake})$
3. $Q_{intake} = imag(S_{intake})$
4. P_{loss} and Q_{loss}

The simulation results of the suggested test system without DG at a base value of 1MVA are displayed in Table 4.

Figure 7 shows the voltage profile of all the 33, 69 and 118-bus tests system. From the figure**,** it is proved that the higher the voltage dependencies more the voltage profile is improved and less power is injected into that bus. Power injection and voltage profiles are highly dependent on non-linear load models. Overall voltage profile is better in commercial load models and hence low power injection in such cases. Performance and validation of the proposed FBS load flow method are as clearly shown in Figure 7, where the proposed method converges efficiently in all the non-linear load models. The figure shows that in base case condition, voltage profile at all the buses is equal to or less than 1 p.u. In a given condition 100% load power is injected into the PQ-bus, therefore, in this case, voltage profile is poor compared to other load models. On the other hand, minimum power is injected into the industrial and commercial load models.

Therefore, fewer power losses are shown in industrial or commercial load models and voltage profile is highly enhanced in all the systems in the base case condition of IND or COM load models.

B. STATISTICAL COMPARISON OF PROPOSED ALGORITHM WITH THE AVAILABLE STATE-OF-ART EAs

In this section, to access the performance of proposed algorithm, three study cases of DG, SC and DG-SC are considered. In small 33-bus and 69-bus system DG, SC allocation consists of 6, 6 dimensions (D), both DG and SC consist of 12 D. Whereas, in 118-bus test system DG and SC consists of 14 D, both the DG and SC allocation length of decision variable is 28. Maximum function evaluation is 3000 in 33 and 69-bus whereas, 6000 in 118-bus network at 30 population size Np. Study cases proposed in this study, systematically investigate the performance of proposed hybrid algorithm, since these exhibit a variety of characteristics such as different dimensions, objective functions, active and reactive power injection, nonlinear nature of objective functions, and various constraints. Additionally, all test cases are independently run 30 times, and the tolerance value for power balance equality constraints is set to 10^{-8} p.u.

Table 5 shows the statistical performance of proposed algorithm compared with the other state-of-the-art evolutionary algorithms (i.e., GA [46], DE [51], PSO [47], ABC [52], CSO [53], FROFI [54], IMODE [48], C^2oDE [50] and SHADE [49]), where FR, Best, Worst, and Avg denote the feasibility ratio, best objective function value, worst objective function value, and average of objective function and computational time complexity values obtained over 30 independent runs. Results in Table 5 proved that proposed algorithm statistically outperforms existing algorithms. Among the ten algorithms in all the cases of 33 and 69 bus tests system GA [46], DE [51], PSO [47], CSO [53], FROFI [54], C^2oDE [50], SHADE [49] and proposed algorithm successfully solve DG, SC and DG-SC allocation problem. Further, in the best value marginal difference is shown, whereas in the worst and mean values of proposed algorithm outperform the other EAs. IMODE consistently fails to find feasible solutions. The proposed algorithm finds better or similar results compared with other EAs. However, in 118-bus it outperforms with marginally higher time complexity. Figure 8 shows the convergence curve of competitive EAs. The convergence curve of proposed algorithm, especially in all the cases of large-scale 118-bus radial distribution systems, is better compared to all other EAs. The simulation results and convergence waveform proved that proposed algorithm can find the global or near-global optimal solution.

C. EFFECT OF LOAD MODELS CONSIDERING DG, SC, AND CUMULATIVE DG-SCC

In this subsection following three case studies are developed to find the optimal DG and SC allocation in radial distribution system.

Case 1. Multiple DGs only
Case 2. Multiple SCBs only
Case 3. Hybrid DG and SC allocation

In the proposed study cases, effect of load models, on the following studies is to be made:

TABLE 4. Results of load flow method in base case without DG/SC.

Test System	Load Model	MVA_{sys}	Total Demand	P_{loss} (kW)	Q_{loss} (KVAr)	V_{min} (bus)
33-bus	'PQ'	4.613	4.369	202.677	135.141	0.913 (18)
	'CI'	4.373	4.161	176.628	117.514	0.919 (18)
	'CZ'	4.176	3.988	156.872	104.175	0.924 (18)
	'IND'	4.258	4.066	161.698	107.486	0.922 (18)
	'COM'	4.170	4.036	154.934	102.873	0.924 (18)
	'RES'	4.223	3.979	159.335	105.852	0.923 (18)
	'Mix'	4.319	4.116	169.955	113.016	0.921 (18)
69-bus	'PQ'	4.903	4.660	224.992	102.158	0.909 (65)
	'CI'	4.660	4.453	191.494	87.792	0.917 (65)
	'CZ'	4.466	4.285	167.159	77.325	0.922 (65)
	'IND'	4.509	4.317	175.081	80.669	0.919 (65)
	'COM'	4.446	4.310	165.041	76.405	0.922 (65)
	'RES'	4.490	4.258	170.821	78.882	0.920 (65)
	'Mix'	4.597	4.397	183.805	84.476	0.918 (65)
118-bus	'PQ'	30.018	28.392	1298.092	978.736	0.869 (77)
	'CI'	28.395	27.009	1102.778	839.288	0.883 (77)
	'CZ'	27.100	25.885	964.631	739.250	0.894 (77)
	'IND'	27.254	26.011	996.408	758.463	0.889 (77)
	'COM'	26.925	25.985	948.365	726.701	0.894 (77)
	'RES'	27.186	25.701	977.882	747.358	0.891 (77)
	'Mix'	27.929	26.604	1054.536	803.408	0.886 (77)

TABLE 5. Statistical results of 33, 69, and 118-bus test systems of constant PQ load model.

33-bus test system															
Algorithm	**DG only**					**SC only**					**DG-SC**				
PP*	'FR'	'Best'	'Worst'	'Avg'	'Time'	'FR'	'Best'	'Worst'	'Avg'	'Time'	'FR'	'Best'	'Worst'	'Avg'	'Time'
Proposed	100	71.457	71.498	71.4586	0.792	100	132.647	133.472	132.674	0.874	100	11.931	12.015	11.950	0.752
'GA'	100	71.457	71.499	71.466	0.608	100	132.649	133.648	133.029	0.646	100	12.540	23.826	14.943	0.586
'PSO'	100	71.499	78.125	74.055	0.564	95.9	132.834	139.311	135.652	0.649	95.2	32.733	111.181	48.970	0.575
'DE'	100	71.839	75.499	73.164	0.598	99.9	133.573	135.110	134.281	0.629	96	19.023	34.782	25.824	0.617
'ABC'	98.0	71.823	75.950	73.353	0.546	99.4	132.662	134.904	133.605	0.597	99.7	17.194	32.418	24.910	0.577
'CSO'	100	71.498	74.865	72.846	0.658	98.8	132.630	136.908	133.945	0.771	99.3	18.548	43.878	30.760	0.614
'FROFI'	100	71.578	75.567	72.975	0.603	97.6	132.434	134.701	133.792	0.663	96.8	18.617	28.416	22.397	0.604
'IMODE'	16.7	71.457	72.218	71.538	0.963	16.7	132.647	133.519	132.799	1.001	16.7	13.930	19.289	15.687	0.842
C^2oDE'	100	71.457	71.764	71.512	1.192	100.0	132.648	133.541	132.811	1.278	100.0	14.171	18.980	16.694	1.436
'SHADE'	100	71.458	72.257	71.641	0.623	100	132.662	134.342	133.061	0.668	100	15.740	24.980	18.656	0.621
69-bus test system															
Proposed	100	69.426	69.426	69.426	0.821	100	145.111	145.111	145.111	0.943	100	4.255	6.003	4.391	0.982
'GA'	100	69.426	71.733	69.778	0.836	100	145.111	146.517	145.406	0.960	100	4.257	9.103	5.910	0.864
'PSO'	99.6	69.801	79.192	74.112	0.789	98	145.378	155.769	149.144	0.931	94.9	12.584	125.033	55.833	0.954
'DE'	100.0	70.037	72.904	71.531	0.876	100.0	145.553	147.133	146.315	1.051	98.4	11.318	30.014	20.102	1.040
'ABC'	99.7	69.540	71.451	70.284	0.825	99.4	145.165	146.331	145.608	0.967	99.8	6.562	22.228	13.119	0.924
'CSO'	100	69.691	75.205	71.594	0.845	100	145.127	150.780	146.378	1.034	99.8	9.617	116.284	30.341	0.988
'FROFI'	99.8	69.749	73.028	70.910	0.851	99	145.261	147.253	146.105	1.057	96.1	9.714	27.391	15.456	0.999
'IMODE'	16.7	69.426	69.801	69.497	1.086	16.7	145.111	145.798	145.168	1.305	16.7	5.136	11.299	7.095	1.242
C^2oDE'	100	69.426	69.867	69.542	1.843	100.0	145.111	145.475	145.176	1.964	100.0	5.527	10.766	7.587	2.058
'SHADE'	100	69.440	70.336	69.784	0.863	100	145.114	145.713	145.225	1.039	100	6.846	14.429	9.098	0.947
118-bus test system															
Proposed	100	539.859	555.954	541.155	2.350	100	834.922	839.330	835.999	2.731	100	127.250	147.645	134.639	2.924
'GA'	100	539.860	568.717	549.423	2.258	100	834.922	846.969	838.906	2.648	100	133.254	171.935	146.393	2.356
'PSO'	100	632.550	758.268	701.322	2.299	100	873.451	985.458	916.564	2.547	100	277.659	474.111	399.804	2.478
'DE'	100	607.275	666.081	640.978	2.568	100	871.350	909.018	892.107	2.611	100	336.689	446.339	389.832	2.837
'ABC'	100	596.279	643.718	619.533	2.564	100	858.745	911.691	889.567	2.550	96.9	346.128	448.187	395.477	2.636
'CSO'	100	583.397	684.179	632.099	2.426	100	862.103	922.078	890.113	2.704	100	291.386	434.974	357.412	2.738
'FROFI'	100	559.969	595.619	583.618	2.467	100	855.280	880.284	869.534	2.566	99.2	260.148	351.047	293.113	2.750
'IMODE'	16.7	541.027	554.015	548.332	2.886	16.7	835.294	850.859	843.041	3.196	16.7	164.257	206.463	182.686	2.763
C^2oDE'	100	541.618	560.869	551.521	5.134	100	837.439	863.951	847.884	5.409	100	199.539	269.487	231.086	5.266
'SHADE'	100	548.238	587.500	569.670	2.412	100	843.680	869.729	859.285	2.837	100	251.750	296.735	274.162	2.665

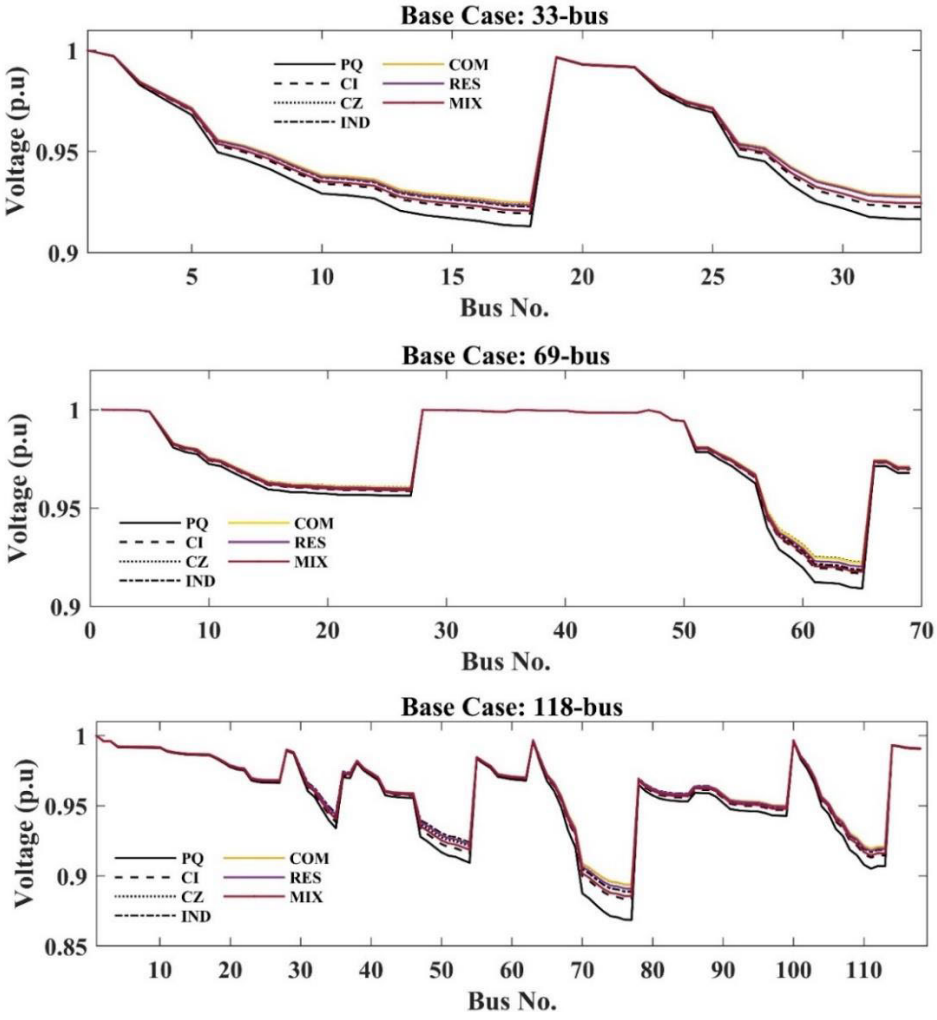

FIGURE 7. Base Case voltage profile of 33, 69, and 118 bus test system.

1. $MVA_{sys} = [(P_{intake} + P_{DG})^2 + (Q_{intake})^2]^{1/2}$
2. $S_{intake} = S_{load} + S_{loss}$
3. $P_{intake} = real(S_{intake})$
4. $Q_{intake} = imag(S_{intake})$
5. Real and reactive power loss reduction
6. Percentage increase (+ve) or decrease (−ve) $MVA^{\pm}{}_{sys} = \left(\frac{MVA_{sys,\ base} - MVA_{sys,\ DG}}{MVA_{sys,\ base}}\right) \times 100$

1) OPTIMAL ALLOCATION OF DG, SC, AND DG-SC EFFECT OF LOAD MODELS ON 33-BUS

In this subsection, the most widely used technical objective functions that are index of active power loss f_1, reactive power loss f_2 and voltage deviation f_3, along with proposed non-linear load models are used to find the optimal DG and SC allocation. Simulation results of proposed hybrid EA for the optimal DG, SC and DG-SC size/locations under the seven different composite voltage-dependent load models are listed in Table 6. Table 6 demonstrates how the appropriate position and size of DG and SC allocation were significantly impacted by the nonlinear load model. In case 1, real and reactive power loss is minimum subject to minimize f_1 and f_2, optimal DG is located at bus [10], [23], [28] and [10], [23], [26] respectively of the 2.786 cumulative DG capacity. However, the voltage deviation index f_3 objective function emphasizes the voltage profile near unity and at near unity injection into the load bus is higher compared to less than unity, therefore, the red color shown in Table 6 gives higher power losses compared to f_1 and f_2. In the PQ load model, injection into load bus is independent of voltage, therefore, f_1 and f_2 reduce more active and reactive losses compared to f_3 in all the cases. Whereas, case 3 reduces more than 95% of power loss (11.9 kW and 9.7 kVAr) in PQ load model and it outperforms case 1 (only DG) and case2 (only SC).

In case 1, minimum active and reactive power losses are shown in industrial load models considering indexes of active f_1 and reactive f_2 power losses that are 56.1 kW and 38.7 kVAr subject to marginal extra injection compared to f_1.

Figure 9 shows the bar chart of proposed parameters and percentage increase and decrease of MVA_{sys} of different load

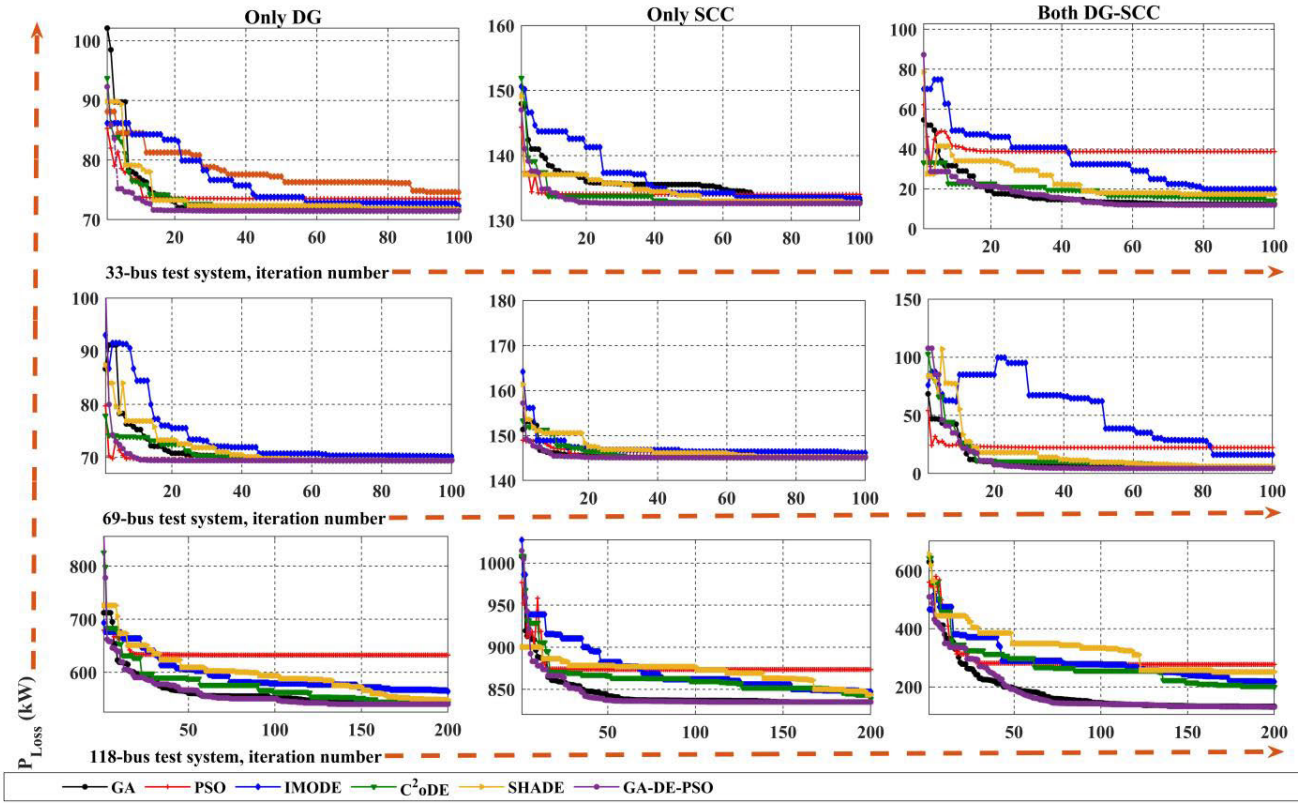

FIGURE 8. Convergence curves of 33, 69, and 118-bus test system.

TABLE 6. Simulation results of cases 1, 2, and 3 of the 33-bus networks.

	Case 1: DG only (MW)		P_{loss}	Q_{loss}	Case 2: SC only (MVAr)		P_{loss}	Q_{loss}	Cas 3: DG (MW) and SC (MVAr)				P_{loss}	Q_{loss}
OF	Site	$\sum_{i=1}^{3} DG_i$			Site	$\sum_{i=1}^{3} SC_i$	kW	KVAr	Site (DG)	$\sum_{i=1}^{3} DG_i$	Site SC	$\sum_{i=1}^{3} SC_i$		
PQf_1	[10,23,28]	2.786	71.7	49.4	[30,23,25]	1.698	140.1	94.3	[28,10,23]	2.786	[10,28,23]	1.725	11.9	9.7
PQf_2	[10,23,28]	2.786	71.7	49.4	[25,23,30]	1.667	140.9	95.0	[23,26,10]	2.786	[23,16,13]	1.725	11.9	9.7
PQf_3	[28,16,21]	2.786	88.2	61.5	[27,25,30]	1.725	147.4	100.7	[21,13,28]	2.786	[11,24,23]	1.725	51.6	38.5
CIf_1	[23,28,10]	2.786	68.1	46.9	[27,23,30]	1.604	127.2	85.2	[23,10,28]	2.783	[23,13,26]	1.725	11.9	9.7
CIf_2	[10,23,28]	2.781	68.1	46.9	[31,15,23]	1.698	126.2	84.5	[13,23,28]	2.592	[23,24,27]	1.459	14.4	11.1
CIf_3	[20,25,17]	2.786	87.6	60.3	[28,25,31]	1.725	136.4	93.2	[32,13,19]	2.786	[19,26,23]	1.725	25.0	18.4
$\boldsymbol{CZf_1}$	[23,28,10]	2.786	64.9	44.7	[10,28,25]	1.724	117.4	78.9	**[10,23,26]**	**2.785**	**[23,10,26]**	**1.724**	**11.6**	**9.5**
$\boldsymbol{CZf_2}$	[28,10,23]	2.715	65.0	44.6	**[32,23,14]**	**1.703**	**113.8**	**76.3**	[10,28,23]	2.761	[28,10,23]	1.725	11.9	9.6
CZf_3	[31,21,19]	2.786	95.1	67.6	[32,25,26]	1.725	124.4	84.2	[33,19,24]	2.786	[23,13,33]	1.724	118.4	107.3
$\boldsymbol{INDf_1}$	**[10,28,23]**	**2.675**	**56.1**	**38.7**	[32,14,25]	1.720	135.3	91.8	[10,26,23]	2.775	[23,13,24]	1.722	11.8	9.6
$\boldsymbol{INDf_2}$	**[10,28,23]**	**2.597**	**56.2**	**38.7**	[25,31,23]	1.666	136.2	91.4	[10,23,28]	2.781	[24,27,23]	1.455	14.2	11.0
$INDf_3$	[25,13,20]	2.786	85.5	59.7	[29,27,33]	1.725	146.6	102.1	[23,13,31]	2.786	[10,13,33]	1.725	53.7	44.7
$COMf_1$	[28,23,10]	2.739	61.5	42.3	[14,32,25]	1.677	119.9	81.1	[10,23,28]	2.780	[23,28,10]	1.724	11.7	9.5
$COMf_2$	[23,10,28]	2.659	61.5	42.3	[23,32,22]	1.690	119.5	79.7	[26,23,10]	2.785	[13,23,26]	1.725	12.0	9.6
$COMf_3$	[25,19,20]	2.786	85.6	59.2	[29,31,25]	1.725	130.1	88.7	[31,29,24]	2.786	[25,31,13]	1.724	191.1	168.8
$RESf_1$	[28,10,23]	2.723	60.1	41.5	[14,32,25]	1.660	126.3	85.5	[23,10,28]	2.786	[10,28,23]	1.725	11.8	9.6
$RESf_2$	[10,28,23]	2.645	60.2	41.4	[23,11,32]	1.701	126.1	85.0	[10,28,23]	2.773	[26,13,23]	1.725	11.7	9.5
$RESf_3$	[21,15,28]	2.786	78.9	55.0	[29,18,32]	1.725	133.8	92.7	[9,29,20]	2.786	[29,22,13]	1.722	227.3	200.7
$Mixf_1$	[28,10,23]	2.786	64.3	44.3	[14,32,25]	1.671	127.9	86.8	[10,23,28]	2.785	[13,26,23]	1.724	11.8	9.6
$Mixf_2$	[10,23,28]	2.714	64.3	44.3	[31,25,23]	1.604	128.8	86.3	[23,26,10]	2.734	[13,23,26]	1.723	12.4	9.8
$Mixf_3$	[20,11,25]	2.786	90.7	63.0	[25,32,20]	1.725	134.7	92.1	[18,29,31]	2.786	[10,13,29]	1.724	55.9	41.3

models. In case 2: only SC injection marginally improves the performance of the power system. Maximum Sc injection can see in 1725 kVAr considering voltage deviation as the objective function. Minimum DG injection is shown in RES load model considering the reactive power index as an objective function. Figure 9 shows the impacts of DG and SC on various nonlinear load models. From Figure 9, it is observed that, in PQ load model, there is a decrease in MVA_{sys} that is due to the optimal placement of DGs and SCs.

On the other hand, in all the remaining load models $\%MVA_{sys}$ is increased. In cases 1 and 3 maximum value of MVA_{sys} is more than 5% is computed in f_3 CZ load model.

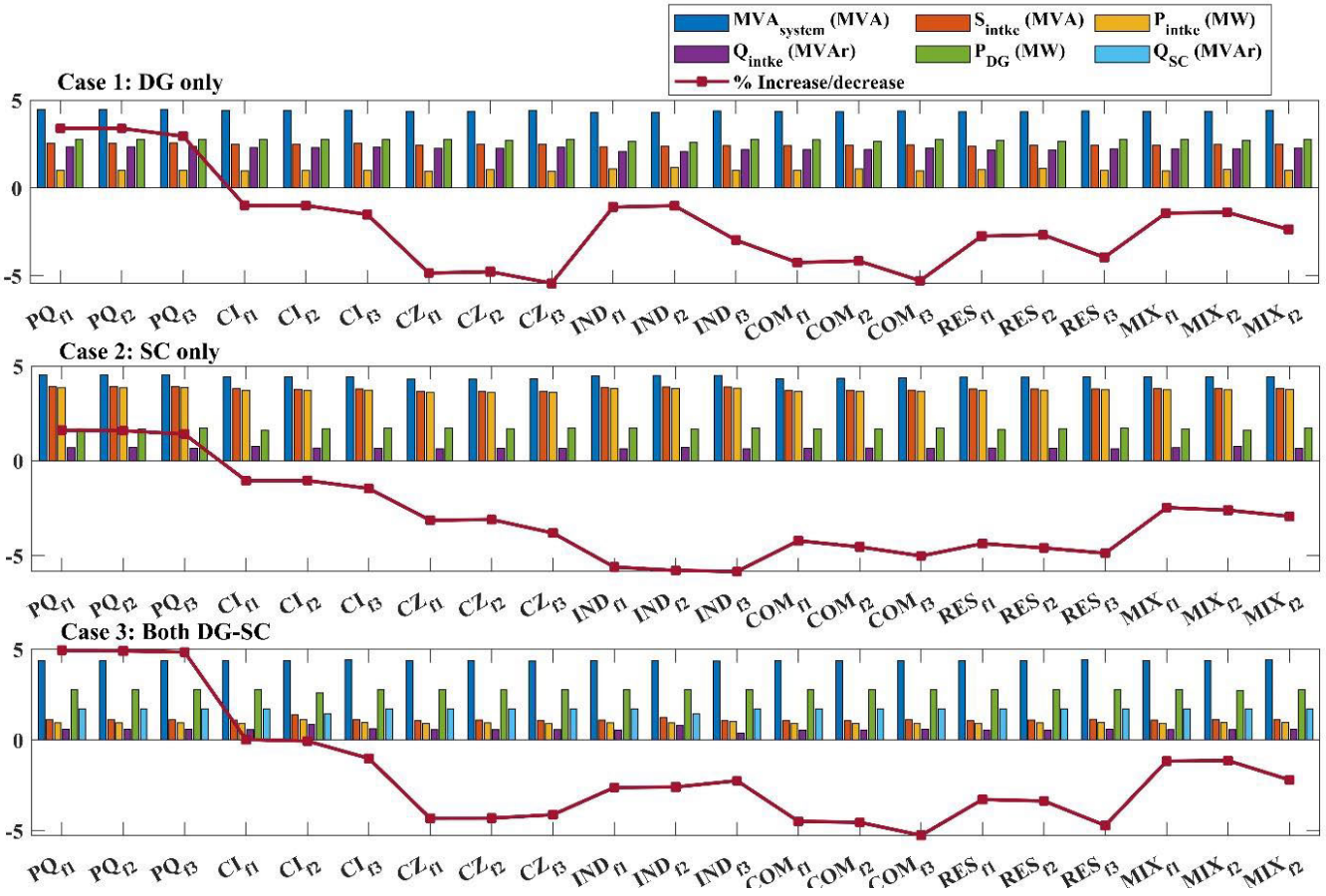

FIGURE 9. Parameters of different load models and percentage increase or decrease of MVA_{sys}.

It means that more than 5% of extra power is injected into the CZ load models to meet the load demand. Whereas, in case 2, maximum MVA_{sys} is injected in f_2 of IND load model. To maximize the benefits of DG and SC allocation, appropriate site and size of DG and SC must be taken into consideration. Otherwise, improper DG and SC allocation that disregards the effects of a real-time voltage-dependent load model results in increased power losses and violates system restrictions.

The voltage profile of the 33-bus test system is shown in Figure 10.

In this figure voltage profiles of all the study cases are within acceptable limits. In case 1 (DG only) voltage profile is equal to marginally less than unity, on the other hand injecting only reactive power in case 2, the voltage profile is marginally enhanced compared to base case condition. It is shown that a highly enhanced voltage profile and hence minimum active and reactive power losses are found in case 3, where, simultaneous DG and SC are employed. In 33-bus test system, higher voltage drop is shown between buses 10-18 and 26-33. Therefore, DG and SC are allocated in the 10-18 and 26-33 buses to enhance voltage profile and reduce power losses. In case3, voltage profile is increased above 1p.u in CZ, COM, RES, and IND load models and optimal site and size considering f_3 an objective function is highly deviated compared to other objective functions. Moreover, simulation results of 33-bus test system proved that enhancement of voltage profile is highly dependent upon the load models. Moreover, with simultaneous integration of DG and SC such as in case 3, active and reactive power loss is highly reduced.

2) EFFECT OF LOAD MODELS ON THE OPTIMAL ALLOCATION OF DG AND DG-SC ON 118-BUS

Simulation results of the proposed hybrid EA for the optimal DG and DG-SC capacities/locations under the seven different composite voltage-dependent load models are listed in Table 7. In this Table in DG allocation, active and reactive power losses are minimum subject to minimize f_1 and f_2, optimal DG is located at bus [112, 34, 99, 104, 55, 63, 70] and [74, 34, 112, 105, 70, 104, 55] respectively of the 12.314 and 12.715 MW of cumulative DG capacity respectively. However, the voltage deviation index f_3 objective function emphasizes the voltage profile near unity and at near unity injection into the load bus is higher compared to less than unity, therefore, the red color shown in Table 7 gives higher power losses compared to f_1 and f_2. In PQ load model, injection into the load bus is independent of voltage, therefore, f_1 and

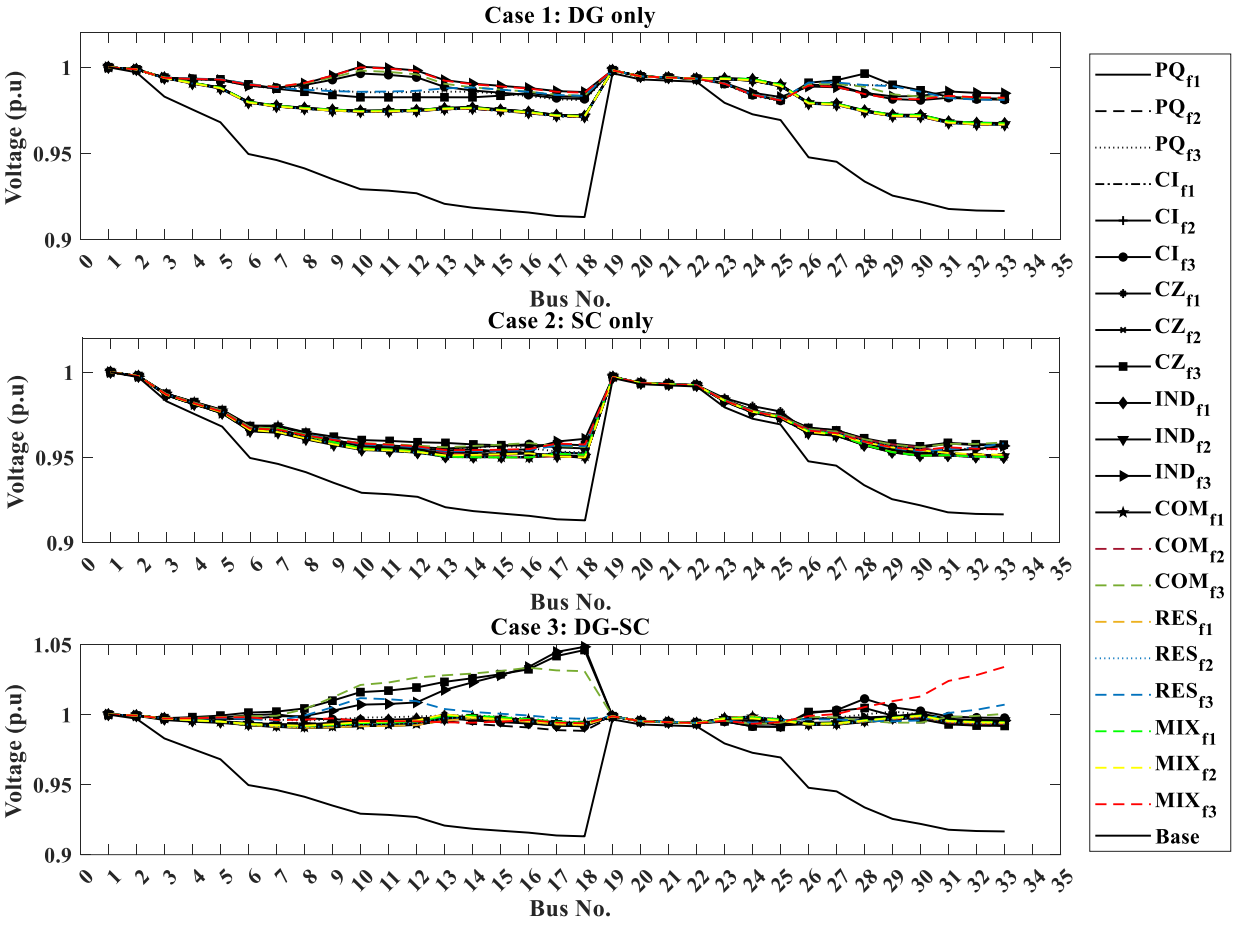

FIGURE 10. Voltage profile of DG, SC, and DG-SC allocation of the 33-bus test system.

TABLE 7. Simulation results of case 1, 2, and 3 of 118-bus network.

	DG only (MW)		P_{loss}	Q_{loss}	DG (MW) and SC (MVAr)				P_{loss}	Q_{loss}
OF	Site	$\sum_{i=1}^{7} DG_i$			Site (DG)	$\sum_{i=1}^{7} DG_i$	Site SC	$\sum_{i=1}^{7} SC_i$		
PQf_1	[112,34,99,104,55,63,70]	12.314	560.8	423.8	[68,98,34,74,105,63,112]	14.012	[41,112,57,104,99,63,34]	11.628	137.7	100.6
PQf_2	[74,34,112,105,70,104,55]	12.715	574.0	426.8	[93,63,34,112,98,42,68]	15.332	[112,34,63,99,30,54,104]	12.231	136.9	89.2
PQf_3	[84,114,99,113,110,36,77]	11.581	716.0	513.6	[89,114,37,45,78,76,99]	17.032	[62,73,104,112,60,35,42]	12.743	558.2	357.4
CIf_1	[70,104,99,42,112,34,63]	12.199	523.9	396.8	[34,41,99,68,112,104,63]	15.035	[68,99,104,112,34,63,41]	11.358	123.6	87.1
CIf_2	[34,63,112,42,104,78,99]	13.093	507.1	383.5	[63,89,34,42,112,93,68]	15.290	[63,112,93,41,104,30,34]	12.391	135.7	87.4
CIf_3	[106,33,110,70,67,116,105]	12.163	616.7	446.2	[99,118,84,76,89,78,63]	17.023	[118,89,60,50,42,79,35]	12.777	455.7	267.2
$\boldsymbol{CZf_1}$	[70,114,63,74,104,78,105]	10.767	503.8	395.9	**[34,78,99,112,63,41,98]**	**14.497**	**[104,68,30,34,99,112,63]**	**12.082**	**121.6**	**86.6**
CZf_2	[42,34,112,104,70,99,63]	12.184	491.8	373.0	[93,89,68,41,34,112,63]	15.497	[54,34,104,99,21,63,112]	12.776	126.0	84.0
CZf_3	[96,70,99,106,109,115,33]	11.598	656.7	471.8	[98,108,106,118,20,34,97]	17.030	[98,118,36,92,93,76,82]	12.770	629.4	345.1
$\boldsymbol{INDf_1}$	**[63,41,34,68,99,104,112]**	**13.093**	**401.0**	**311.3**	[112,63,34,41,104,78,99]	14.507	[68,34,104,63,99,21,112]	12.552	121.3	88.7
$\boldsymbol{INDf_2}$	**[42,78,63,99,34,89,112]**	**12.789**	**403.5**	**306.2**	**[34,63,98,93,78,41,112]**	**15.022**	**[41,63,99,30,112,34,104]**	**12.059**	**126.0**	**81.7**
$INDf_3$	[62,99,113,93,46,114,55]	11.486	497.2	364.6	[115,102,64,93,78,49,42]	17.032	[48,76,61,64,115,102,103]	12.780	776.6	594.4
$COMf_1$	[112,42,99,63,78,34,104]	12.829	444.8	338.2	[63,41,104,99,78,34,112]	14.458	[63,68,104,34,99,112,30]	12.029	121.0	86.4
$COMf_2$	[34,68,104,99,42,63,112]	13.390	445.9	338.9	[63,89,41,93,112,34,78]	15.016	[112,104,34,99,63,21,54]	12.781	125.5	83.7
$COMf_3$	[104,55,105,98,33,117,84]	12.315	597.3	417.5	[76,104,50,105,58,118,68]	16.997	[22,71,117,92,118,73,106]	12.778	696.8	452.3
$RESf_1$	[104,80,63,99,78,114,34]	11.179	448.9	350.6	[104,41,112,34,68,63,99]	14.985	[41,68,104,63,99,34,112]	11.185	121.0	85.5
$RESf_2$	[99,112,104,63,34,42,78]	12.909	434.7	330.2	[41,93,63,68,112,34,89]	15.540	[99,104,34,30,54,112,63]	12.035	126.8	81.9
$RESf_3$	[73,104,96,89,111,105,102]	10.652	560.7	423.5	[58,77,114,99,24,76,98]	17.032	[76,43,50,48,78,23,33]	12.780	560.8	397.7
$MIXf_1$	[34,112,78,42,104,99,63]	12.887	471.3	357.5	[112,41,89,63,99,68,34]	15.143	[99,104,41,68,112,63,34]	11.294	122.8	86.1
$MIXf_2$	[42,63,99,112,68,104,34]	13.483	472.3	358.1	[41,93,63,34,30,112,89]	16.076	[105,34,42,74,89,112,41]	11.401	147.1	91.3
$MIXf_3$	[114,64,98,77,36,99,59]	10.892	543.6	419.1	[47,78,112,98,63,76,50]	17.032	[80,69,106,105,48,67,112]	12.781	660.4	366.7

f_2 reduces more active and reactive losses compared to f_3 in all the cases. Whereas, case3 reduces more than 90% of active and reactive power losses (137.7 and 100.6) in PQ load model and it outperforms case 1 (only DG) and case 2 (only SC). In case 1, minimum active and reactive power losses are shown in industrial (IND) load models considering

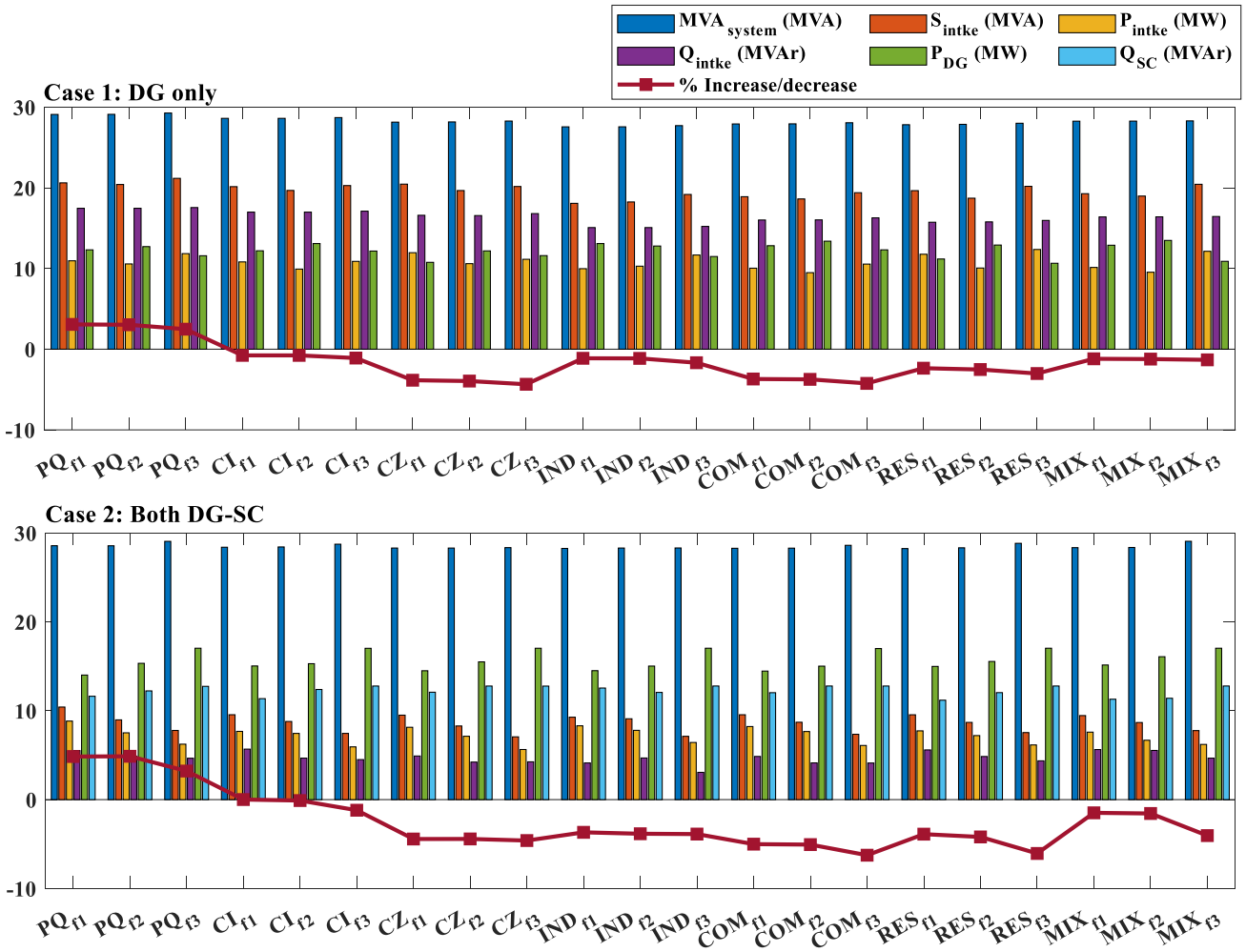

FIGURE 11. Impacts of different load models and percentage increase or decrease of MVA system.

indexes of active f_1 and reactive f_2 power losses that are 401kW and 306.2 kVAr subject to marginally higher injection compared to f_1. Active power injection of DG is increased when both DG and SC are integrated. Figure 11 shows the bar chart of proposed parameters and the percentage increase and decrease of MVA_{sys} of different load models.

From Figure, it is observed that, in the PQ load model, there is a decrease in MVA_{sys}, and due to placement of DGs and SCs. Furthermore, MVA of the DISCO also gets reduced in PQ load models. Hence, when constant load model is assumed, the reduction in and is directly translated as the reduction in overall system MVA which gives an erroneous indication of higher benefits of DG placement. However, negative values of $\%MVA_{sys}$ regarding base case condition, as shown in Figure 11, indicates that extra MVA_{sys} is required to meet nonlinear load models. In DG-SC allocation percentage increase of MVA_{sys} is more than 7% is computed in RES and COM load model subject to minimizing f_3 objective functions.

It means that more than 7% of extra power is injected into the RES and COM load models to meet the load demand. Figure 12 shows the voltage profile of 118-bus test system. Figure shows that voltage level at all the buses is within acceptable limits. DG allocation only, the voltage profile is equal to or marginally less than unity in f_1 and f_2. The figure of voltage profile shows that the enhanced voltage profile and hence minimum active and reactive power losses are found in DG-SC allocation, where, simultaneous DG and SC are employed. Moreover, f_3 emphasize the improvement of voltage profile at the same time extra-MVA is consumed due to the higher value of voltage. Usually, DG and SC integration causes improvement in voltage profile and reduction in losses in a constant PQ load model. However, there would be a dire need for care of voltage enhancement that causes extra injection into the voltage-dependent nonlinear load buses that lead towards inappropriate DG and SC allocation. In DG-Sc allocation, the voltage profile is increased above 1p.u in CZ, COM, RES, and IND load models and

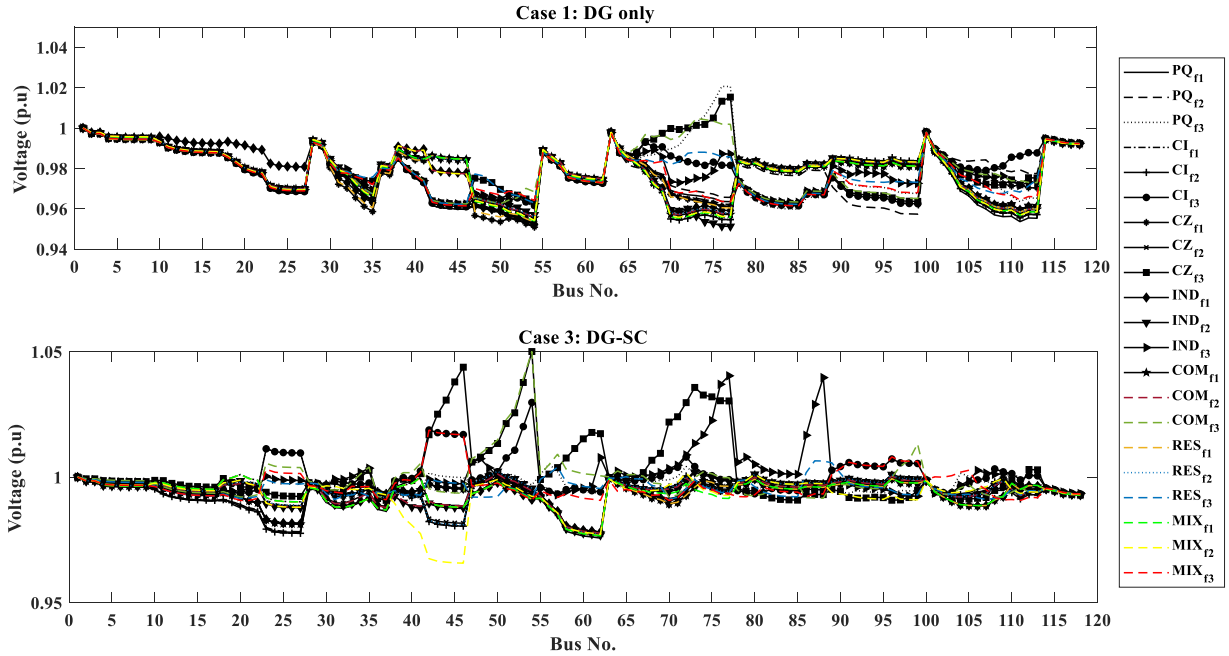

FIGURE 12. Voltage profile of all the study cases of 118-bus test system.

TABLE 8. Cost analysis of DG_SC allocation in 33-bus tests system.

Quantity/ Load Model	PQ	CI	CZ	IND	COM	RES	MIX
	1314.4/16	793/5	1088.1/23	658.8/3	245.0/26	1444.5/15	1475.3/11
P_{DG} (kW)/bus	756.3/8	651.4/20	837.9/10	1039.5/23	1901.7/15	209.0/28	1213.3/29
	712.8/19	1321.8/14	850.5/16	1087.1/28	638.1/10	1123.2/10	82.7/17
	934.0/27	131.2/32	0	518.6/3	1070.0/5	879.1/11	814.5/19
Q_{SC} (kVAr)/bus	582.8/30	468.4/29	836.6/11	349.2/32	272.1/15	427.4/25	430.4/29
	186.8/17	1074.9/8	871.2/23	843.1/27	351.2/19	411.8/8	256.8/18
$\sum_{i=1}^{3} P_{DG}$ (MW)	2.7835	2.7662	2.7764	2.7853	2.7848	2.7767	2.7713
$\sum_{i=1}^{3} Q_{SC}$ (MW)	1.7035	1.6745	1.7078	1.7108	1.6933	1.7183	1.5016
V_{min} (p.u)/bus	0.983 (25)	0.973 (31)	0.969 (18)	0.984 (25)	0.968 (18)	0.967 (18)	0.972 (18)
V_{max} (p.u)/bus	1.003 (08)	1.000 (01)	1.003 (30)	1.016 (17)	1.000 (01)	1.000 (01)	1.024 (33)
P_{Loss} (kW)	39.4	39.4	21.7	30.6	39.3	32.7	48.4
Q_{Loss} (kVAr)	30.5	33.1	16.8	25.1	31.6	26.5	42.1
C_{SS} (* 1000 $)	50.9	50.5	47.9	48.4	46.9	47.8	54.5
C_{DG} (* 1000 $)	182.4	182.2	182.3	182.4	182.4	182.3	182.3
C_{SC} (* 1000 $)	8.2	8.1	8.3	8.3	8.2	8.3	7.3
C_{TOT} (* 1000 $)	241.5	240.9	238.5	239.1	237.5	238.4	244.2
C_{Emiss} (* 1000 t/h)	1988.1	1954.6	1880.9	1957.6	1882.0	1928.3	1944.7
MVA_{sys} (MVA)	4.419	4.381	4.349	4.370	4.326	4.351	4.374
S_{intake} (MVA)	1.1557	1.1482	1.0897	1.1011	1.0665	1.0857	1.2397
P_{intake} (MW)	0.9709	0.9545	0.9185	0.9560	0.9191	0.9417	0.9497
Q_{intake} (MVAr)	0.6270	0.6381	0.5862	0.5465	0.5411	0.5403	0.7968
% increase/decrease	4.2033	-0.1864	-4.15325	-2.6278	-3.74187	-3.02932	-1.25619

optimal site and size considering f_3 an objective function is highly deviated compared to other objective functions. Moreover, simulation results of 118-bus test system proved that enhancement of the voltage profile is highly dependent upon the load models. Results clearly show the performance and superiority of proposed algorithm to solve complex DG and SC allocation problems. Moreover, simultaneous integration of DG and SC can highly reduce active and reactive power loss.

D. MULTIOBJECTIVE ECONOMIC AND ENVIRONMENTAL IMPACTS OF DG AND SC ALLOCATION IN 33 AND 118-BUS SYSTEM

In this part, the cost analysis and other performance parameters of assigning a 3-DG and a 3-SC to the 33-bus system are investigated. The findings are shown in Table 8. For all load models, the min/max voltage values are restricted to the standard limitations of ±5%. The reduction of real and reactive loss with DG-SC allocations in the 33-bus network

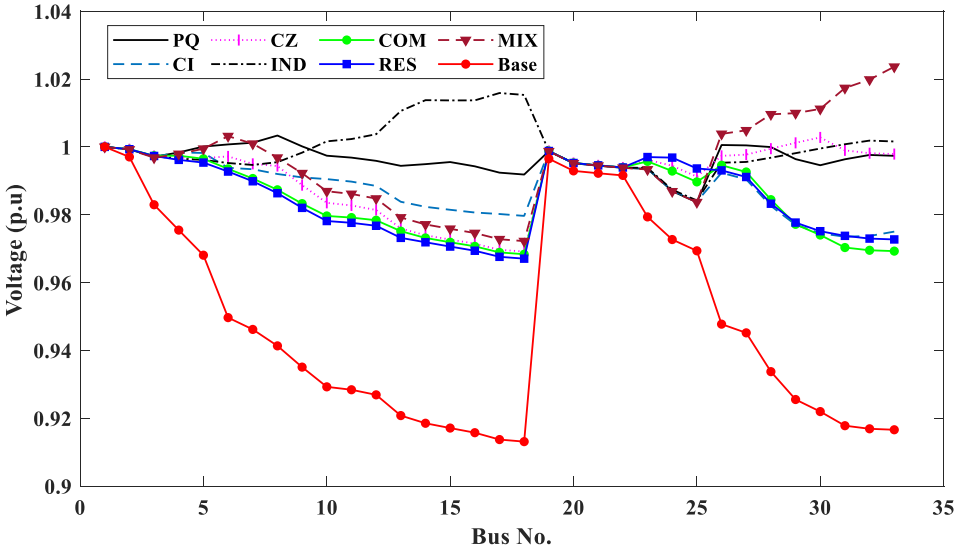

FIGURE 13. Voltage profile of 33-bus test system, Simultaneous DG, and SC allocation.

TABLE 9. Cost analysis of DG_SC allocation in 118-bus tests system.

Quantity/Load Model	PQ	CI	CZ	IND	COM	RES	MIX
	2.9265 (89)	2.9393 (68)	2.1951 (112)	2.7751 (12)	2.9976 (96)	2.8486 (86)	2.8525 (96)
	2.8572 (20)	1.9837 (105)	2.9972 (30)	1.9571 (49)	2.4594 (68)	2.7048 (07)	2.1909 (83)
	1.4747 (106)	1.7558 (37)	2.9456 (70)	2.9657 (109)	2.0971 (35)	2.7272 (35)	2.9169 (23)
P_{DG} (kW)/bus	1.9448 (93)	1.8605 (116)	2.5946 (105)	2.4598 (105)	1.1864 (73)	1.8964 (104)	1.7844 (54)
	2.4974 (34)	2.9992 (30)	1.6679 (23)	1.2302 (71)	2.3007 (113)	1.6479 (06)	1.7411 (44)
	2.9436 (112)	2.8338 (98)	2.3538 (20)	2.6708 (68)	2.9961 (12)	2.5504 (84)	2.4865 (98)
	2.3076 (44)	2.6535 (15)	2.2474 (36)	2.8964 (104)	2.9555 (99)	2.6488 (63)	2.9626 (64)
	2.5639 (112)	2.8300 (109)	2.1727 (23)	2.5274 (84)	1.7865 (80)	2.2254 (14)	2.5651 (24)
	0.9453 (106)	0.5791 (62)	2.0015 (86)	0.5760 (115)	1.2961 (57)	2.4583 (55)	1.7569 (43)
	0.6795 (90)	2.8267 (74)	1.7835 (111)	2.4659 (52)	1.8611 (52)	1.9968 (77)	2.0080 (84)
Q_{SC} (kVAr)/bus	1.8965 (84)	1.4090 (57)	1.4818 (116)	0.3335 (43)	1.4733 (47)	0.3782 (40)	0.8759 (21)
	2.8347 (21)	1.7467 (104)	1.5828 (104)	1.6097 (34)	2.0459 (102)	1.3991 (15)	2.3778 (34)
	1.2219 (63)	0.4562 (90)	1.6105 (29)	2.4194 (114)	2.6905 (105)	2.4144 (74)	1.6976 (42)
	1.6026 (80)	1.5410 (39)	1.5201 (36)	1.3708 (70)	0.9290 (72)	1.4697 (59)	1.2259 (70)
$\sum_{i=1}^{7} P_{DG}$ (MW)	16.9517	17.0257	17.0017	16.9553	16.9928	17.0242	16.9350
$\sum_{i=1}^{7} Q_{SC}$ (MVAr)	11.7445	11.3885	12.1529	11.3020	12.0826	12.3419	12.5070
V_{min} (p.u)/bus	0.9746 (99)	0.9691 (99)	0.9665 (46)	0.9774 (27)	0.9779 (27)	0.9661 (46)	0.9634 (54)
V_{max} (p.u)/bus	1.0096 (112)	1.0120 (41)	1.0110 (70)	1.0185 (74)	1.0111 (76)	1.0102 (96)	1.0182 (98)
P_{Loss} (kW)	199.7	232.4	199.5	204.8	205.4	278.3	279.0
Q_{Loss} (kVAr)	136.0	153.7	133.9	150.0	140.2	195.1	185.4
C_{SS} (* 1000 $)	354.76	355.91	325.44	355.36	327.41	317.64	323.56
C_{DG} (* 1000 $)	317.01	317.71	317.49	317.05	317.40	317.70	316.85
C_{SC} (* 1000 $)	54.08	52.46	55.95	52.06	55.63	56.81	57.57
C_{TOT} (* 1000 $)	725.86	726.09	698.87	724.47	700.44	692.15	697.98
C_{Emiss} (* 1000 t/h)	12199.75	11750.22	11486.70	12150.68	11621.31	11841.73	12113.61
MVA_{sys} (MVA)	28.63	28.46	28.27	28.38	28.27	28.25	28.41
S_{intake} (MVA)	8.06	8.09	7.40	8.08	7.44	7.22	7.35
P_{intake} (MW)	5.96	5.74	5.61	5.93	5.68	5.78	5.92
Q_{intake} (MVAr)	5.43	5.70	4.82	5.48	4.81	4.32	4.37
% increase/decrease	4.6115	-0.2462	-4.3294	-4.1371	-5.0013	-3.8992	-1.7099

is listed in Table 8. The minimum losses depend on the load model type. Minimum values of active and reactive power losses are computed in CZ load model. The minimum voltage found in RES load model is 0.967 p.u @18 bus and maximum bus voltage has appeared in MIX load model which is 1024 p.u @33 bus. Total operating cost C_{TOT} is maximum obtained in COM load model with 237.5 thousand dollars. In the PQ load model, there is 4.203% of MVA capacity is reduced due to DG and SC allocation. However, other nonlinear load models consume extra MVA capacity from the system. Out of which, maximum extra MVA capacity is consumed in CZ load model which is 4.1532%. The minimum value of emission is 1880.9 thousand tons per hour can be seen in the MIX load model. It is clear how the

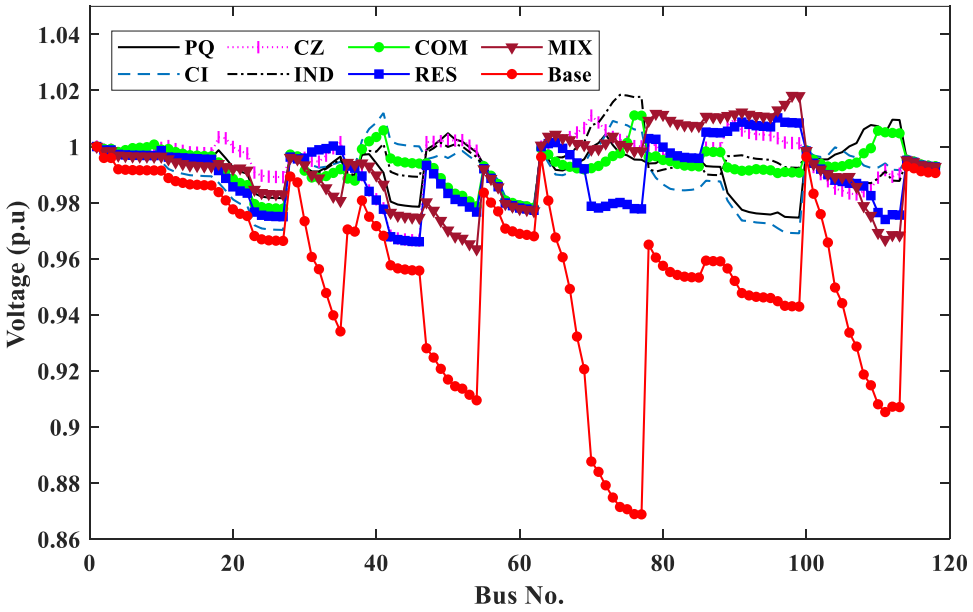

FIGURE 14. Voltage profile of 118-bus test system, simultaneous DG, and SC allocation.

load model affects the voltage profile. As illustrated in Figure 13, the voltage profiles for the integration of three DG and SC pairs are drawn and compared with the base case.

For all forms of nonlinear loads, it is obvious that integrating the DG and SC pairings improves the voltage profile. Additionally, the voltage profile is further improved by expanding the DG and SC pair. All case studies' voltage profiles fall within the accepted ranges. In the remaining part, the cost analysis and other performance factors of assigning a 7-DG and a 7-SC to the 118-bus system are investigated. The findings are shown in Table 9.

The reduction of active and reactive power losses with different DG/SC allocations in the 118-bus distribution network is listed in Table 9. As can be seen, the reduction of losses depends on the demand type. Minimum values of active and reactive power losses are computed in CZ load model which are 199.5 kW and 133.9 kVAr respectively. The minimum voltage found in MIX load model is 0.9634 p.u @54 bus and the maximum bus voltage that appeared in IND load model is 1.018 p.u @74 bus.

Total operating cost C_{TOT} is maximum obtained in CI load model with 726.09 thousand dollars. In PQ load model there is 4.6115% of MVA capacity is reduced due to DG and SC allocation. However, other nonlinear load models consume extra MVA capacity from the system. Out of which, maximum extra MVA capacity consumed in COM load model is 5.0013%. The minimum value of emission is 12199.75 thousand tons per hour can be seen in PQ load model. The effect of the load type on the voltage profile is apparent. The voltage profiles for the cases of integrating seven DG and SC pairs are drawn and compared to the base case, as shown in Figure 14. The voltage profile for all nonlinear load types are improved by integrating the DG and SC pairs, it is obvious. Further improving the voltage profile is achieved by increasing the DG and SC pair. The voltage profiles for each case study are within the accepted ranges.

VI. CONCLUSION

In this paper, a new fast and efficient forward-backward sweep (FBS) load flow method based on branch and bus ordering is successfully applied to solve the load flow problem considering nonlinear voltage-dependent composite load models for various small (33-bus) to large scale (118-bus) radial distribution system. Recently, several state-of-the-art EAs are employed to solve optimal site and size of DG and SC allocation problems. Several multi-methods and multi-operator-based algorithms have been proposed for solving optimization problems. Generally, their performance is better than other algorithms that are based on a single operator and/or algorithm. Therefore, a new hybrid EA based on various state-of-the-art operators such as GA, DE, and PSO is designed and applied to solve optimal DG and SC allocation problems. Moreover, statistical results show that the performance of proposed algorithm is better or almost comparable to other state-of-the-art EAs. Various technical objective functions (index of active and reactive power loss and voltage deviation index) are considered to show the impacts of non-linear load models. The index of active and reactive power loss emphasizes the loss reduction, whereas, the index of voltage deviation emphasizes the enhancement of the voltage profile. From the simulation results, it is shown that DG and SC allocation problem is multi-objective. Therefore, in this paper weighted sum multi-objective technical, economic, and environmental objective functions are considered. The gathered results demonstrate that the proposed

method significantly lowers the cost of energy supplied by the grid, total operating cost, and power losses. On the other hand, system stability and the voltage profile have both improved. Consequently, it can be stated that the suggested methodology has considerable fiscal and technological benefits and may be used to address optimization issues in various distribution networks.

REFERENCES

[1] A. Khodabakhshian and M. H. Andishgar, "Simultaneous placement and sizing of DGs and shunt capacitors in distribution systems by using IMDE algorithm," *Int. J. Elect. Power Energy Syst.*, vol. 82, pp. 599–607, Nov. 2016.

[2] M. A. Abdelkader, M. A. Elshahed, and Z. H. Osman, "An analytical formula for multiple DGs allocations to reduce distribution system losses," *Alexandria Eng. J.*, vol. 58, no. 4, pp. 1265–1280, Dec. 2019.

[3] S. Maheswarapu, "A solution to multi-objective optimal accommodation of distributed generation problem of power distribution networks: An analytical approach," *Int. Trans. Electr. Energy Syst.*, vol. 29, no. 10, Oct. 2019, Art. no. e12093.

[4] J. A. Sa'ed, M. Amer, A. Bodair, A. Baransi, S. Favuzza, and G. Zizzo, "A simplified analytical approach for optimal planning of distributed generation in electrical distribution networks," *Appl. Sci.*, vol. 9, no. 24, p. 5446, Dec. 2019.

[5] S. N. G. Naik, D. K. Khatod, and M. P. Sharma, "Analytical approach for optimal siting and sizing of distributed generation in radial distribution networks," *IET Gener., Transmiss. Distrib.*, vol. 9, no. 3, pp. 209–220, 2015.

[6] R. Viral and D. K. Khatod, "An analytical approach for sizing and siting of DGs in balanced radial distribution networks for loss minimization," *Int. J. Electr. Power Energy Syst.*, vol. 67, pp. 191–201, May 2015.

[7] A. Ehsan and Q. Yang, "Optimal integration and planning of renewable distributed generation in the power distribution networks: A review of analytical techniques," *Appl. Energy*, vol. 210, pp. 44–59, Jan. 2018.

[8] S. Elsaiah, M. Benidris, and J. Mitra, "Analytical approach for placement and sizing of distributed generation on distribution systems," *IET Gener., Transmiss. Distrib.*, vol. 8, no. 6, pp. 1039–1049, Jun. 2014.

[9] D. Q. Hung, N. Mithulananthan, and R. C. Bansal, "Analytical expressions for DG allocation in primary distribution networks," *IEEE Trans. Energy Convers.*, vol. 25, no. 3, pp. 814–820, Sep. 2010.

[10] A. Naderipour, Z. Abdul-Malek, M. Hajivand, Z. M. Seifabad, M. A. Farsi, S. A. Nowdeh, and I. F. Davoudkhani, "Spotted hyena optimizer algorithm for capacitor allocation in radial distribution system with distributed generation and microgrid operation considering different load types," *Sci. Rep.*, vol. 11, no. 1, p. 2728, Feb. 2021.

[11] Y. M. Shuaib, M. S. Kalavathi, and C. C. Rajan, "Optimal capacitor placement in radial distribution system using gravitational search algorithm," *Int. J. Electr. Power Energy Syst.*, vol. 64, pp. 384–397, Jan. 2015.

[12] K. Balu and V. Mukherjee, "Siting and sizing of distributed generation and shunt capacitor banks in radial distribution system using constriction factor particle swarm optimization," *Electric Power Compon. Syst.*, vol. 48, nos. 6–7, pp. 697–710, Apr. 2020.

[13] A. Noori, Y. Zhang, N. Nouri, and M. Hajivand, "Multi-objective optimal placement and sizing of distribution static compensator in radial distribution networks with variable residential, commercial and industrial demands considering reliability," *IEEE Access*, vol. 9, pp. 46911–46926, 2021.

[14] A. Selim, S. Kamel, F. Jurado, J. A. P. Lopes, and M. Matos, "Optimal setting of PV and battery energy storage in radial distribution systems using multi-objective criteria with fuzzy logic decision-making," *IET Gener., Transmiss. Distrib.*, vol. 15, no. 1, pp. 135–148, Jan. 2021.

[15] E. A. Almabsout, R. A. El-Sehiemy, O. N. U. An, and O. Bayat, "A hybrid local search-genetic algorithm for simultaneous placement of DG units and shunt capacitors in radial distribution systems," *IEEE Access*, vol. 8, pp. 54465–54481, 2020.

[16] D. Q. Hung, N. Mithulananthan, and R. C. Bansal, "Analytical strategies for renewable distributed generation integration considering energy loss minimization," *Appl. Energy*, vol. 105, pp. 75–85, May 2013.

[17] M. B. Jannat and A. S. Savić, "Optimal capacitor placement in distribution networks regarding uncertainty in active power load and distributed generation units production," *IET Gener., Transmiss. Distrib.*, vol. 10, no. 12, pp. 3060–3067, Sep. 2016. [Online]. Available: https://digital-library.theiet.org/content/journals/10.1049/iet-gtd.2016.0192

[18] P. P. Biswas, R. Mallipeddi, P. N. Suganthan, and G. A. J. Amaratunga, "A multiobjective approach for optimal placement and sizing of distributed generators and capacitors in distribution network," *Appl. Soft Comput. J.*, vol. 60, pp. 268–280, Nov. 2017.

[19] A. A. A. El-Ela, R. A. El-Sehiemy, and A. S. Abbas, "Optimal placement and sizing of distributed generation and capacitor banks in distribution systems using water cycle algorithm," *IEEE Syst. J.*, vol. 12, no. 4, pp. 3629–3636, Dec. 2018.

[20] R. S. Rao, K. Ravindra, K. Satish, and S. V. L. Narasimham, "Power loss minimization in distribution system using network reconfiguration in the presence of distributed generation," *IEEE Trans. Power Syst.*, vol. 28, no. 1, pp. 317–325, Feb. 2013.

[21] A. Ali, M. U. Keerio, and J. A. Laghari, "Optimal site and size of distributed generation allocation in radial distribution network using multi-objective optimization," *J. Mod. Power Syst. Clean Energy*, vol. 9, no. 2, pp. 404–415, 2021.

[22] A. Eid, "Cost-based analysis and optimization of distributed generations and shunt capacitors incorporated into distribution systems with nonlinear demand modeling," *Expert Syst. Appl.*, vol. 198, Jul. 2022, Art. no. 116844.

[23] M. G. Hemeida, S. Alkhalaf, A.-A.-A. Mohamed, A. A. Ibrahim, and T. Senjyu, "Distributed generators optimization based on multi-objective functions using manta rays foraging optimization algorithm (MRFO)," *Energies*, vol. 13, no. 15, p. 3847, Jul. 2020, doi: 10.3390/EN13153847.

[24] S. Abdelhady, A. Osama, A. Shaban, and M. Elbayoumi, "A real-time optimization of reactive power for an intelligent system using genetic algorithm," *IEEE Access*, vol. 8, pp. 11991–12000, 2020.

[25] A. Eid, "Performance improvement of active distribution systems using adaptive and exponential PSO algorithms," *Int. Rev. Electr. Eng.*, vol. 16, no. 2, pp. 147–157 2021.

[26] M. M. Ansari, C. Guo, M. S. Shaikh, N. Chopra, I. Haq, and L. Shen, "Planning for distribution system with grey wolf optimization method," *J. Electr. Eng. Technol.*, vol. 15, no. 4, pp. 1485–1499, Jul. 2020.

[27] A. Eid, S. Kamel, A. Korashy, and T. Khurshaid, "An enhanced artificial ecosystem-based optimization for optimal allocation of multiple distributed generations," *IEEE Access*, vol. 8, pp. 178493–178513, 2020.

[28] L. F. Ochoa, A. Padilha-Feltrin, and G. P. Harrison, "Evaluating distributed generation impacts with a multiobjective index," *IEEE Trans. Power Del.*, vol. 21, no. 3, pp. 1452–1458, Jul. 2006.

[29] W. El-Khattam, Y. Hegazy, and M. Salama, "An integrated distributed generation optimization model for distribution system planning," in *Proc. IEEE Power Eng. Soc. Gen. Meeting*, 2005, p. 2392.

[30] P. Chiradeja and R. Ramakumar, "An approach to quantify the technical benefits of distributed generation," *IEEE Trans. Energy Convers.*, vol. 19, no. 4, pp. 764–773, Dec. 2004.

[31] D. Singh, R. K. Misra, and D. Singh, "Effect of load models in distributed generation planning," *IEEE Trans. Power Syst.*, vol. 22, no. 4, pp. 2204–2212, Nov. 2007.

[32] Y. G. Hegazy, M. M. A. Salama, and A. Y. Chikhani, "Adequacy assessment of distributed generation systems using Monte Carlo simulation," *IEEE Trans. Power Syst.*, vol. 18, no. 1, pp. 48–52, Feb. 2003.

[33] A. Arif, Z. Wang, J. Wang, B. Mather, H. Bashualdo, and D. Zhao, "Load modeling—A review," *IEEE Trans. Smart Grid*, vol. 9, no. 6, pp. 5986–5999, Nov. 2018.

[34] W. Price, "Bibliography on load models for power flow and dynamic performance simulation," *IEEE Trans. Power Syst.*, vol. 10, no. 1, pp. 523–538, Feb. 1995.

[35] D. T. Rizy, J. S. Lawler, J. B. Patton, and W. R. Nelson, "Measuring and analyzing the impact of voltage and capacitor control with high speed data acquisition (distribution system)," *IEEE Trans. Power Del.*, vol. 4, no. 1, pp. 704–714, Jan. 1989.

[36] S. Arnborg, G. Andersson, D. J. Hill, and I. A. Hiskens, "On influence of load modelling for undervoltage load shedding studies," *IEEE Trans. Power Syst.*, vol. 13, no. 2, pp. 395–400, May 1998.

[37] P. D. P. Reddy, V. C. V. Reddy, and T. G. Manohar, "An efficient distribution load flow method for radial distribution systems with load models," *Int. J. Grid Distrib. Comput.*, vol. 11, no. 3, pp. 63–78, Mar. 2018.

[38] A. Ahmed, M. F. N. Khan, I. Khan, H. Alquhayz, M. A. Khan, and A. T. Kiani, "A novel framework to determine the impact of time varying load models on wind DG planning," *IEEE Access*, vol. 9, pp. 11342–11357, 2021.
[39] A. M. El-Zonkoly, "Optimal placement of multi-distributed generation units including different load models using particle swarm optimization," *Swarm Evol. Comput.*, vol. 1, no. 1, pp. 50–59, Mar. 2011.
[40] A. Ali, M. U. Keerio, and N. H. Mugheri, "Constrained composite differential evolution search for optimal site and size of distributed generation along with reconfiguration in radial distribution network," *Mehran Univ. Res. J. Eng. Technol.*, vol. 39, no. 4, pp. 705–718, Oct. 2020.
[41] D. Rajicic, R. Ackovski, and R. Taleski, "Voltage correction power flow," *IEEE Trans. Power Del.*, vol. 9, no. 2, pp. 1056–1062, Apr. 1994.
[42] D. Das, D. P. Kothari, and A. Kalam, "Simple and efficient method for load flow solution of radial distribution networks," *Int. J. Elect. Power Energy Syst.*, vol. 17, no. 5, pp. 335–346, Oct. 1995.
[43] M. Kefayat, A. L. Ara, and S. A. N. Niaki, "A hybrid of ant colony optimization and artificial bee colony algorithm for probabilistic optimal placement and sizing of distributed energy resources," *Energy Convers. Manage.*, vol. 92, pp. 149–161, Mar. 2015.
[44] A. M. Shaheen, R. A. El-Sehiemy, and S. M. Farrag, "Adequate planning of shunt power capacitors involving transformer capacity release benefit," *IEEE Syst. J.*, vol. 12, no. 1, pp. 373–382, Mar. 2018.
[45] D. H. Wolper and W. G. Macready, "No free lunch theorems for optimization," *IEEE Trans. Evol. Comput.*, vol. 1, no. 1, pp. 67–82, Apr. 1997.
[46] K. Deb, K. Sindhya, and T. Okabe, "Self-adaptive simulated binary crossover for real-parameter optimization," in *Proc. 9th Annu. Conf. Genetic Evol. Comput.*, Jul. 2007, pp. 1187–1194.
[47] A. Zeinalzadeh, Y. Mohammadi, and M. H. Moradi, "Optimal multi objective placement and sizing of multiple DGs and shunt capacitor banks simultaneously considering load uncertainty via MOPSO approach," *Int. J. Electr. Power Energy Syst.*, vol. 67, pp. 336–349, May 2015.
[48] K. M. Sallam, S. M. Elsayed, R. K. Chakrabortty, and M. J. Ryan, "Improved multi-operator differential evolution algorithm for solving unconstrained problems," in *Proc. IEEE Congr. Evol. Comput. (CEC)*, Jul. 2020, pp. 1–8.
[49] R. Tanabe and A. Fukunaga, "Success-history based parameter adaptation for differential evolution," in *Proc. IEEE Congr. Evol. Comput.*, Jun. 2013, pp. 71–78.
[50] B. Wang, H. Li, J. Li, and Y. Wang, "Composite differential evolution for constrained evolutionary optimization," *IEEE Trans. Syst., Man, Cybern., Syst.*, vol. 49, no. 7, pp. 1482–1495, Jul. 2019.
[51] H. Li and Q. Zhang, "Multiobjective optimization problems with complicated Pareto sets, MOEA/D and NSGA-II," *IEEE Trans. Evol. Comput.*, vol. 13, no. 2, pp. 284–302, Apr. 2009.
[52] D. Karaboga, "An idea based on honey bee swarm for numerical optimization," Tech. Rep., 2005.
[53] R. Cheng and Y. Jin, "A competitive swarm optimizer for large scale optimization," *IEEE Trans. Cybern.*, vol. 45, no. 2, pp. 191–204, Feb. 2015.
[54] Y. Wang, B.-C. Wang, H.-X. Li, and G. G. Yen, "Incorporating objective function information into the feasibility rule for constrained evolutionary optimization," *IEEE Trans. Cybern.*, vol. 46, no. 12, pp. 2938–2952, Dec. 2016.

AAMIR ALI received the B.E., M.E., and Ph.D. degrees in electrical engineering from the Quaid-e-Awam University of Engineering Science and Technology (QUEST), Nawabshah, Pakistan. He is currently an Assistant Professor with the Department of Electrical Engineering, QUEST. His main research interests include power system optimization, grid-connected and islanded operation of distributed generation, smart grids, and multiobjective evolutionary algorithms.

GHULAM ABBAS received the B.Eng. degree in electrical engineering from the Quaid-e-Awam University of Engineering Science and Technology (QUEST), Nawabshah, Pakistan, in 2017, and the M.Eng. degree in electrical engineering from Southeast University, Nanjing, China, in 2019, where he is currently pursuing the Ph.D. degree in electrical engineering. His research interests include distributed generations' integration, planning, and optimization.

MUHAMMAD USMAN KEERIO was born in Nawabshah, Pakistan, in December 1965. He received the bachelor's degree in electrical (power) engineering from the Mehran University of Engineering and Technology, Jamshoro, in 1991, the master's degree in control engineering from NUST, Karachi, in 2002, and the Ph.D. degree in controls and robotics from the Beijing Institute of Technology, China, in 2008. His research interests include electrical and control engineering, curriculum development, institutional accreditation, neural networks, and optimization.

SOHRAB MIRSAEIDI (Senior Member, IEEE) received the Ph.D. degree in electrical engineering from Universiti Teknologi Malaysia (UTM), Malaysia, in 2016. He furthered his Postdoctoral Fellowship with the Department of Electrical Engineering, Tsinghua University, China, from 2016 to 2019. He is currently an Associate Professor with the School of Electrical Engineering, Beijing Jiaotong University, China. He has authored more than 50 articles and two books in the field of microgrids and large-scale power systems and has been involved in several national research projects in China. His research interests include control and protection of large-scale hybrid AC/DC grids and microgrids, power system stability, and application of power electronics in power systems. He is a Senior Member of IET, CIGRE, and the Chinese Society of Electrical Engineering.

SHAHR ALSHAHR received the B.S. degree in electrical engineering from Jouf University, Aljouf, Saudi Arabia, in 2011, and the M.S. and Ph.D. degrees in electrical and computer engineering from Western Michigan University, Kalamazoo, MI, USA, in 2015 and 2021, respectively. He is currently an Assistant Professor with Jouf University. His research interests include smart grids, microgrids, and control systems.

AHMED ALSHAHIR received the B.S. degree in electrical engineering from Jouf University, Aljouf, Saudi Arabia, in 2012, the M.S. degree in electrical and computer engineering from Southern Illinois University, Carbondale, IL, USA, in 2015, and the Ph.D. degree in electrical engineering and computer science from The University of Toledo, Toledo, OH, USA, in 2021. He is currently an Assistant Professor with Jouf University. His research interests include smart grids, stability, control systems, and energy storage systems.